LUND UNIVERSITY

Influence of core divisome proteins on cell division in Streptomyces venezuelae ATCC 10712

Cantlay, Stuart; Sen, Beer Chakra; Flärdh, Klas; McCormick, Joseph R.

Published in:
Microbiology (Reading, England)

DOI:
10.1099/mic.0.001015

2021

Document Version:
Peer reviewed version (aka post-print)

Link to publication

Citation for published version (APA):
Cantlay, S., Sen, B. C., Flärdh, K., & McCormick, J. R. (2021). Influence of core divisome proteins on cell division in Streptomyces venezuelae ATCC 10712. *Microbiology (Reading, England)*, *167*(2). https://doi.org/10.1099/mic.0.001015

Total number of authors:
4

General rights
Unless other specific re-use rights are stated the following general rights apply:
Copyright and moral rights for the publications made accessible in the public portal are retained by the authors and/or other copyright owners and it is a condition of accessing publications that users recognise and abide by the legal requirements associated with these rights.
• Users may download and print one copy of any publication from the public portal for the purpose of private study or research.
• You may not further distribute the material or use it for any profit-making activity or commercial gain
• You may freely distribute the URL identifying the publication in the public portal

Read more about Creative commons licenses: https://creativecommons.org/licenses/

Take down policy
If you believe that this document breaches copyright please contact us providing details, and we will remove access to the work immediately and investigate your claim.

LUND UNIVERSITY

PO Box 117
221 00 Lund
+46 46-222 00 00

© Stuart Cantlay, Beer Chakra Sen, Klas Flärdh and Joseph R. McCormick. The definitive peer reviewed, edited version of this article is published in Microbiology (Reading). 2021 Feb;167(2). doi: 10.1099/mic.0.001015.

Influence of core divisome proteins on cell division in *Streptomyces venezuelae* ATCC 10712

Stuart Cantlay[1,#], Beer Chakra Sen[2], Klas Flärdh[2] and Joseph R. McCormick[1,*]

[1] *Department of Biological Sciences, Duquesne University, Pittsburgh, PA 15282, USA*

[2] *Department of Biology, Lund University, 223 62 Lund, Sweden*

[#]*Current address: Department of Biological Sciences, West Liberty University, West Liberty, WV 26074, USA*

**Corresponding author*

Department of Biological Sciences, Duquesne University, Pittsburgh, PA 15282, USA

Tel: (+1) 412 396 4775

Email: mccormick@duq.edu

Running Title: Divisome genes in *S. venezuelae*

Keywords: divisome, septation, sporulation, spore, morphological development

ABSTRACT

The sporulating, filamentous, soil bacterium *S. venezuelae* ATCC 10712 differentiates under submerged and surface growth conditions. In order to lay a solid foundation for the study of development-associated division for this organism, a congenic set of mutants was isolated, individually deleted for a gene encoding either a cytoplasmic (i.e., *ftsZ*) or core inner membrane (i.e., *divIC*, *ftsL*, *ftsI*, *ftsQ*, *ftsW*) component of the divisome. While *ftsZ* mutants are completely blocked for division, single mutants in the other core divisome genes resulted in partial, yet similar, blocks in sporulation septum formation. Double and triple mutants for core divisome membrane components displayed phenotypes that were similar to the single mutants, demonstrating that the phenotypes were not synergistic. Division in this organism is still partially functional without multiple core divisome proteins, suggesting that perhaps other unknown lineage-specific proteins perform redundant functions. In addition, by isolating an *ftsZ2p* mutant with an altered -10 region, the conserved developmentally controlled promoter was also shown to be required for sporulation-associated division. Finally, microscopic observation of FtsZ-YFP dynamics in the different mutant backgrounds led to the conclusions that the initial assembly of regular Z rings does not *per se* require the tested divisome membrane proteins, but that stability of Z rings is dependent on the divisome membrane components tested. The observation is consistent with the interpretation that Z ring instability likely results from and further contributes to the observed defects in sporulation septation in mutants lacking core divisome proteins.

INTRODUCTION

Since the 1960s, *Streptomyces coelicolor* A3(2) has been used as the model system to study the filamentous sporulating soil bacteria in the genus *Streptomyces* [1]. The streptomycetes are true mycelial organisms of ecological importance, and are responsible for the synthesis of many important biologically active compounds, including a wide range of antibiotics [2]. To facilitate dispersal in the environment, and to enable long-term survival, streptomycetes produce semi-dormant spores. Spores are formed as part of a complex developmental life cycle, in which the streptomycete initially grows vegetatively as branching hyphae while nutrients are available, forming a vegetative mycelium, also referred to as substrate mycelium. Eventually, specialized spore-forming aerial hyphae emerge on the colony surface. The apical parts of such aerial hyphae are partitioned into chains of prespores via synchronous formation of several tens of cell division septa in each hypha, and thereafter prespores mature to form pigmented and thick-walled spores with condensed nucleoids and a hydrophobic outer surface layer, before being released into the environment (reviewed in e.g. [3-5]). When conditions are favorable, spores germinate and grow to form a new mycelium. The formation of aerial mycelium and spores is governed by a regulatory cascade of transcription factors that has been studied mainly in *S. coelicolor*, but more recently much progress has been made in mapping the developmental regulatory networks in the new model organism *Streptomyces venezuelae* [3-5].

Cell division and its regulation are of central importance in the *Streptomyces* life cycle, which involves two distinct types of division. Both types are formed by a typical bacterial cell division machinery, organized by the tubulin homolog FtsZ [6, 7]. In vegetatively growing hyphae, cell division is infrequent and gives rise to widely-spaced hyphal cross-walls. Intriguingly, vegetative hyphae can grow even in the absence of such cross-walls and cell division is not essential for proliferation of these organisms; the key cell division gene *ftsZ* is dispensable for growth and viability in *S. coelicolor* and *S. venezuelae* [8, 9]. The *ftsZ*-null mutants do not make cross-walls at all, but can still grow as branching hyphae. On the other hand, cell division is absolutely essential for spore formation. The septa that divide aerial hyphae into prespore compartments are formed by the same *ftsZ*-dependent core cell division machinery as the vegetative cross-walls. However, sporulation septa differ from hyphal cross-walls. Structurally, sporulation septa are thicker,

eventually leading to full constriction and separation of daughter cells, and sporulation septatation is subject to spatial and temporal regulation [10].

Cell division genes are developmentally regulated and directly controlled by several of the key transcriptional regulators that govern morphological differentiation and sporulation. For example, *ftsZ* has a developmentally-regulated promoter, *ftsZ2p*, that is critical for spore formation [11]. This promoter is repressed by the master regulator BldD in complex with cyclic di-GMP; c-di-GMP-bound BldD negatively controls many important genes related to aerial mycelium formation and sporulation [12, 13]. In *S. venezuelae*, both the *ftsZ2p* promoter and promoters for cell division genes *ftsW*, *ftsK*, and *sepF2* are activated by the proteins WhiA and WhiB, which presumably act as a complex that controls a large regulon of genes involved in spore formation [14, 15]. In addition, *ssgB* and, indirectly, *ssgA* are controlled by the developmental regulator BldM [16]. SsgA and SsgB belong to an actinobacteria-specific protein family and affect selection of septation sites in *S. coelicolor* [17]. Finally, two dynamin-like proteins are involved in septation specifically in sporulating aerial hyphae, and developmental upregulation of the corresponding genes, *dynA* and *dynB*, depends on the sporulation-specific GntR-family regulator WhiH in *S. venezuelae* [18].

The bacterial cell division process is primarily controlled at the level of assembly of FtsZ into cytokinetic polymers and their formation of a ring-shaped pattern, the Z ring, which serves to recruit and organize most other proteins involved in cell constriction and septum formation [19-21]. Interestingly, streptomycetes, as well as Actinobacteria in general, lack obvious homologs of most of the proteins that are known to regulate Z-ring formation, including MinC, MinD, SulA, Noc, or to stabilize FtsZ polymers or tether them to the cytoplasmic membrane, like FtsA and ZipA [6, 7]. The exception is SepF, which links FtsZ to membranes and facilitates Z-ring formation in Gram-positive bacteria like *Bacillus subtilis* [22], and which is present as three homologues in *S. venezuelae* [18]. The regulation of Z-ring assembly in *Streptomyces* remains poorly understood. During sporulation, SsgA and SsgB proteins have been reported to mark the sites of Z-ring formation in *S. coelicolor* [17], and DynA and DynB are recruited to septation sites and help stabilize Z rings in *S. venezuelae* [18]. DynA and DynB interact with each other, and DynB also interacts with both SsgB and one of the three SepF proteins in *S. venezuelae* [18]. Analyses with two-hybrid systems have further suggested that the three SepF proteins interact with each other,

SepF interacts with FtsZ, and SepF2 interacts with both DynB and SsgB [18], indicating a sophisticated protein interaction network affecting Z-ring assembly. Additional proteins have been suggested to affect this critical step in cell division, including SepG and CrgA, but details still remain unclear [23, 24].

Once formed, the Z ring recruits further division proteins that collectively are referred to as the divisome. Present in streptomycetes are orthologues of conserved divisome proteins FtsQ, FtsL, and DivIC(FtsB), which are known to form a complex with a structural and/or regulatory role in *Escherichia coli* and *B. subtilis* [19, 25, 26], and FtsW and FtsI, which encode a peptidoglycan transglycosylase of the shape, elongation, division, and sporulation (SEDS) family, and a cognate penicillin-binding protein with transpeptidase activity, respectively [27]. In addition, the DNA-translocase FtsK and ABC-transporter proteins FtsEX are encoded by streptomycete genomes [7]. Genetic studies in *S. coelicolor* show that none of these proteins are essential for growth or viability, which is consistent with the finding that cell division is dispensable in streptomycetes. However, although mutants for *ftsQ*, *ftsL*, *divIC*, *ftsW*, and *ftsI* are largely defective in spore formation, none of these genes are absolutely needed for cell division, with all mutants being able to form hyphal cross-walls and some sporulation septa [28-31]. For the last four genes, the mutant phenotypes were found to be conditional, leading to suppression of the septation defect on minimal medium or low osmolarity medium. Mutants lacking *ftsK* or *ftsEX* show apparently regular sporulation septation, but *ftsK* mutants have a defect in chromosome stability, presumably related to the role of FtsK in clearing trapped chromosomes from the closing septa [7, 32-34].

The fact that *Streptomyces* cell division is non-essential, developmentally regulated, disconnected from vegetative growth, and involves previously unknown mechanisms for control of septum formation, make streptomycetes attractive model systems to study the division process and its regulation [6, 7]. This distinction is further accentuated by the recent development of live cell imaging systems in the new model organism *S. venezuelae* that allow time-lapse visualization of the cell division in great detail through the entire life cycle [3, 35]. In order to further establish *S. venezuelae* as a cell division model system, we report the isolation and characterization of null mutants for key cell division genes *ftsZ*, *ftsQ*, *ftsL*, *divIC*, *ftsW*, and *ftsI* for this organism, and we clarify the effect of late divisome components on assembly of Z rings and cell division in *S. venezuelae*.

METHODS

Bacterial strains and growth conditions

The *S. venezuelae* strains used in this study were derived from *S. venezuelae* strain ATCC 10712, acquired from Dr. Colin Stuttard (Dalhousie University, Halifax, Canada) (Table S1). *S. venezuelae* strains were cultivated at 30°C on maltose yeast extract medium (MYM) agar plates or in MYM liquid medium [36], as described by Bush *et al*. [14]. *S. venezuelae* transconjugants were selected on either MYM or R2S agar after interspecies conjugation, as described previously [37]. Culture conditions and antibiotics followed previously described procedures for streptomycetes [38]. *E. coli* strain TG1 was used for cloning, construction, and propagation of vectors [39]. *E. coli* strain BW25113/pIJ790 [40-43] was used to create cosmid derivatives containing insertion-deletion mutations. *E. coli* strain ET12567/pUZ8002 was used for mobilization of *oriT*-containing cosmids and plasmids into *S. venezuelae* [37, 38]. *E. coli* strain BT340 was used to express yeast Flp recombinase in *E. coli* to excise antibiotic resistance markers flanked by *FRT* sites [44]. Culture conditions, antibiotic concentrations and genetic manipulations generally followed those previously described for *E. coli* [39].

Plasmids and general DNA techniques

Plasmids and cosmids used in this study are listed in Table S2. DNA restriction and modifying enzymes were used according to the manufacturer's recommendation (New England BioLabs). Phusion DNA polymerase (Thermo Fisher Scientific) was used according to the manufacturer's instructions. *S. venezuelae* total DNA preparations were obtained using the Wizard genomic DNA purification kit (Promega). λRED-mediated recombineering, modified for *Streptomyces*, was used in *E. coli* to replace *S. venezuelae* genes on cosmids with mutagenic linear DNA cassettes [43]. Apramycin-resistance gene cassette [*oriT acc(3)IV*] was amplified by PCR from plasmid pIJ773. The oligonucleotide primers used in this study are listed in Table S3. When necessary, the *bla* gene of the cosmid backbone was replaced by recombineering with a *bla* homology-flanked *oriT acc(3)IV*-cassette from pIJ799. Plasmid pMS82 was used to create genetic complementation plasmids for site-specific integration in the chromosome at the ΦBT1 attachment site [45]. DNA

sequences of unmarked in-frame deletions were verified using BigDye cycle sequencing analyzed on an ABI 3130 Prism Genetic Analyzer (Applied Biosystems).

Isolation of strains mutant for cell division genes

Using PCR product-directed recombineering of cosmid inserts [43], insertion-deletion mutations were created in which all or crucial portions of the coding regions of *S. venezuelae* division genes were replaced with an apramycin-resistance cassette (*oriT acc(3)IV*) from pIJ773 (Table S2). Care was taken when designing the 3' endpoints of in-frame deletions to minimize the potential polar effects on expression of the downstream co-transcribed gene(s). Mutagenized cosmids were confirmed by restriction enzyme digestion and PCR amplification with primers flanking the introduced mutations. These mutagenized cosmids were introduced into *S. venezuelae* by interspecies conjugation and marked null mutants, generated by double homologous recombination events, were identified among primary transformants by their apramycin-resistant, kanamycin-sensitive phenotypes. Genomic DNA from mutant candidates was analyzed by PCR amplification using primers flanking the mutations.

Most mutations were designed to introduce unique *Xba*I and *Spe*I sites flanking the *oriT acc(3)IV* cassette that was inserted into cosmids to generate the marked insertion-deletions. These restriction sites facilitated the isolation of unmarked deletion mutant strains. The mutagenized cosmids were digested with *Xba*I and *Spe*I and re-ligated, removing the *oriT acc(3)IV* cassette, leaving a 6 bp in-frame scar with the sequence of ACTAGA. Alternatively, the antibiotic-resistance cassette was removed by site-specific recombination resulting in an 81-bp *frt* scar for unmarked *ftsZ* and *ftsI* mutations. Subsequently, a linear *oriT acc(3)IV* cassette was used to replace the *bla* gene on the cosmid backbone allowing conjugation into *S. venezuelae* and selection of exconjugants by apramycin resistance marker in the vector backbone. Primary exconjugants generated by a single homologous recombination incident were screened by PCR for gene conversion events in which resident wild type alleles were replaced with the introduced unmarked mutagenized ones. Generally, 5-10% of exconjugants had undergone gene conversion events. Exconjugants that were homozygous for the mutant allele were re-streaked without selection to allow loss of integrated cosmids and progeny colonies were screened for apramycin sensitivity, indicating intramolecular homologous recombination events and the loss of the cosmid. All of the mutants chosen for further

characterization were checked by PCR amplification from genomic DNA with primers flanking the introduced mutation to confirm the presence of only the unmarked deletion allele. Double mutants were constructed by introducing marked insertion-deletion mutations into unmarked single mutants, as described above for isolating single mutants. A triple mutant for *ftsL*, *ftsQ* and *divIC* was isolated in a similar fashion from an unmarked double mutant strain. A double mutant strain for the adjacent *ftsL* and *ftsI* genes was obtained by combining recombineering primers used for single mutation isolation (i.e., using the 5' *ftsL* primer and the 3' *ftsI* primer). The resulting Δ*ftsIL*::*apra* mutation was introduced into the chromosome in the same way as for single mutant isolation.

For generation of a non-sporulating strain by manipulating the developmentally controlled *ftsZ2p*, the TAGTGT residues of the -10 motif on cosmid Sv-4-G01 were replaced with an *oriT acc(3)IV* cassette flanked by introduced *Spe*I and *Xba*I sites. Restriction digestion of the mutagenized cosmid with *Spe*I and *Xba*I and re-ligation left ACTAGA in place of the native -10 sequence. Exconjugants were selected as described above for unmarked mutations and identified by a PCR analysis using oligonucleotides specific for each of the two promoter sequences.

Construction of genetic complementation plasmids

For genetic complementation, a series of DNA fragment inserts were generated from cosmids by restriction digestion or amplification by PCR (Fig. 1a and Fig. S8) and cloned into site-specific integration vectors pMS82. The resulting plasmids were introduced into *S. venezuelae* mutant strains by conjugation and integrated *in trans* into the chromosome at the ΦBT1 attachment site.

Construction of strains expressing fluorescent FtsZ-YPet fusion proteins

Plasmid pKF351, carrying and *ftsZ-ypet* fusion in a vector that integrates at the ΦC31 attachment site [46], was introduced into relevant mutants by interspecies conjugation, as described above.

Microscopy

For phase-contrast microscopy, bacteria were grown as confluent patches on MYM agar. Cover slips were touched to the surface of sporulated patches and material lifted was mounted on pads of 1% agarose in PBS. Samples were visualized using a Nikon Eclipse E400 with a Nikon 100x 1.25 NA oil immersion objective and a MicroPublisher 5.0 RTV high resolution CCD camera (Qimaging).

For staining of cell wall and nucleoids, cultures were grown on MYM agar or in MYM liquid medium, and samples were fixed in ice-cold methanol for 5 minutes, washed twice in PBS and mounted in 100 μg ml^{-1} propidium iodide (Molecular Probes) and 10 μg ml^{-1} WGA-FITC (Molecular Probes) in 50% glycerol. Fixed and stained samples were then spotted onto pads of 2% agarose in PBS and sealed with petroleum jelly. Fluorescence imaging was done with a Leica SP2 TCS confocal microscope using a Leica 63x 1.4 NA glycerin immersion objective.

In order to visualize fluorescent FtsZ-YPet fusion protein, cells were grown in liquid MYM, harvested and fixed with 2.28% formaldehyde and 0.018% glutaraldehyde, washed in PBS, and mounted on 1% agarose in PBS. To follow FtsZ dynamics, microfluidics-based time-lapse microscopy was performed using the CellASIC ONIX system and B04A-03 microfluidic plates (Merck Millipore), as described previously [35, 47]. The live-cell time lapse experiments were repeated twice for each strain. Imaging was performed on a Zeiss AxioObserver.Z1 microscope with Zeiss Plan-Apochromat 100×/1.4 Oil Ph3 objective, ZEN software (Zeiss) and an ORCA Flash 4.0 LT camera (Hamamatsu). Images and movies were processed using ImageJ/Fiji [48].

For Transmission Electron Microscopy (TEM), cells were grown as lawns on MYM agar and fixed in 2.5% glutaraldehyde in 0.05 M cacodylate buffer (pH 7.2) and incubated for 1 h in 2% osmium tetroxide. Cells were dehydrated by successive transfer in 5 steps from 50% to 100% ethanol. Cells were washed in propylene oxide and then in a 1:1 solution of propylene oxide and Spurr's before being incubated in Spurr's resin overnight at 60°C. Thin sections were stained with 2% uranyl acetate and 1% lead citrate. Samples were visualized using a JEOL JEM-1210 equipped with a Hamamatsu Orca-HR CCD camera.

RESULTS AND DISCUSSION

Generation of *ftsZ*-null mutants

The earliest acting divisome protein FtsZ is required for cell division and viability in most bacteria. Previously, it had been demonstrated that *ftsZ*-null strains could be isolated for *S. coelicolor* [8]. However, it was not clear whether this would be a general property of streptomycetes. Therefore, the procedure for isolating a deletion-insertion mutation for *S. coelicolor ftsZ* was replicated in *S. venezuelae* by replacing 844 bp, starting 16 bp upstream of the *ftsZ* start codon, with an apramycin-resistance cassette (Fig. 1a). The mutants described in this paper were isolated in *S. venezuelae* ATCC 10712 acquired from Dr. Colin Stuttard (Dalhousie University, Halifax, Canada). In three independent experiments, we were able to isolate *S. venezuelae* null mutants for *ftsZ*. However, in contrast to the majority of the other cell division mutants isolated in *S. venezuelae* (described below), obtaining the *ftsZ*-null mutants was not as straightforward. The initial *ftsZ*-null mutant colonies grew very slowly after selection on conjugation plates, therefore, waiting up to 8 days before picking colonies was necessary to identify these mutants as “specks” or “flecks” on the agar surface. These primary mutant colonies on conjugation plates did not increase in size upon prolonged incubation, nor did they sector. Subsequently, mutants were re-streaked several times on selective media. *ftsZ*-null mutants were unhealthy and grew slowly on the nalidixic acid-containing medium used for counter-selection of the conjugation donor *E. coli*, perhaps contributing to the difficulty when isolating them initially and, similarly, when introducing an empty vector as control for genetic complementation studies (see below). Once nalidixic acid counter-selection was no longer needed, the single colonies were uniform in appearance and the phenotype was stable. Colonies of the purified *ftsZ*-null strains appeared on plates at similar incubation times relative to the wild type, however, plating efficiency was much lower (Figs. S1 and S2); mature colonies were smaller and took much longer to develop an aerial mycelium, as judged by the surface of the colonies becoming white. Isolated independent strains had similar microscopic phenotypes and the insertion-deletion mutation of *ftsZ* was confirmed by PCR from genomic DNA. One representative strain was picked for further analysis (DU500). As expected, western blot analysis verified that FtsZ was not detected in a whole cell extract from DU500 (Fig. S3). As anticipated, phase-contrast and TEM microscopic analyses of the *ftsZ*-null mutant grown on agar showed that aerial hyphae did not differentiate to produce spores and the vegetative hyphae

were devoid of the normal cross-walls (Figs. 1b and c). The *ftsZ*-null mutant was also completely blocked in both cell division and spore production when grown in liquid cultures and little cell material accumulated for the mutant under these growth conditions (data not shown). To confirm that the observed division phenotype was the result of the introduced mutation, genetic complementation studies were carried out. A restriction fragment containing *ftsQ*, *ftsZ* and the native *ftsZ* promoters in the intergenic region between the genes was integrated at the chromosomal *att*ΦBT1 site (pJS8; Fig. 1a). The complementation vector rescued the division phenotype of the *ftsZ*-null mutants, as judged by phase-contrast microscopy (Fig. 1b), as well as restored growth and colony size on agar medium (Figs. S2 and S3). We conclude that the deletion-insertion mutation is not polar on downstream gene expression, and FtsZ-dependent cell division is dispensable for growth and viability of *S. venezuelae*. Nonetheless, an unmarked *ftsZ*-null strain was also generated and it had an identical microscopic phenotype as the insertion-deletion mutant, but was not used further in this study (DU665, data not shown). The fact that an unmarked null mutant can be isolated by gene conversion (see Methods) argues that the *ftsZ* mutants are difficult to distinguish from background on primary conjugation plates, not that they can only be isolated by very strong selection for marker replacement by double homologous recombination.

Using the same procedure that is described above, we have also isolated an *ftsZ*-null mutant (DU669) in the *S. venezuelae* strain NRRL B-65442 obtained from Dr. Mark Buttner (John Innes Centre, Norwich, UK) [49]. The mode of growth of this *ftsZ*-null mutant DU699 (NRRL B-65442 background) in the absence of cell division and hyphal cross-walls has been described elsewhere [9]. As observed for other cell division mutants (data not shown), the macroscopic and microscopic phenotypes of *ftsZ*-null mutants in the two independent wild type backgrounds were essentially indistinguishable and could be genetically complemented, revealing no overt differences at the phenotypic level between the *S. venezuelae* parent strains obtained from different sources. All experiments described in the rest of this paper were carried out in the ATCC 10712 strain background. (Nonetheless, about a dozen core divisome mutant strains were also isolated in the NRRL B-65442 background. Their strain designations and genotypes are listed in Table S1.)

The developmentally regulated promoter of *ftsZ* is required for sporulation-associated cell division in *S. venezuelae*

For *S. coelicolor*, three promoters for *ftsZ* have been mapped to the 288 bp intergenic region between *ftsZ* and *ftsQ*, and one of them, *ftsZ2p*, is developmentally regulated [11]. It has been shown that BldD, a transcriptional regulator that plays a key role in *Streptomyces* development, binds to the developmentally-regulated *ftsZ2p* promoter and acts to repress expression of *ftsZ* during vegetative growth [12]. In *S. venezuelae* it has been shown that expression of *ftsZ* is dependent on WhiA and WhiB, which are transcriptional regulators required for the transition from growth of aerial hyphae to sporulation [14, 15]. ChIP experiments indicated that a WhiA binding target lies around 158 bp from the predicted start codon of *ftsZ* [14], and in this region is a sequence that is identical to the -10 region TAGTGT of the *S. coelicolor ftsZ2p* [11] and *S. griseus* P_{spo} [50]. The intergenic region upstream of *ftsZ* is highly conserved between *S. coelicolor* and *S. venezuelae* with sequence conservation at the three mapped promoter regions, including the *ftsZ2p* promoter (Fig. S4a). To test whether the importance of this developmental promoter for sporulation was also retained in *S. venezuelae*, a strain was generated that was mutant for this presumed *ftsZ2p* promoter region. In the unmarked mutant, the TAGTGT residues at the -10 region of this presumed promoter were changed to ACTAGA (Fig. 4b). The resulting strain (DU523) had reduced plating efficiency compared to the wild type, but grew robustly and formed an abundant aerial mycelium (Fig. S1). However, the *ftsZ2p* mutant was unable to efficiently convert the aerial hyphae to spore chains during growth on solid medium, and mature spores were observed much less frequently compared to the wild type. Instead, longer spore-like compartments of irregular length were produced from aerial hyphae (Fig. 1b). Thus, this promoter mutant can form functional division septa that result in complete division events with cell separation that lead to formation of spore-like aerial hyphal fragments. However as shown by the absence of regularly septated spore chains, the mutant has a greatly reduced frequency of cell division compared to wild type. The phenotype of the *S. venezuelae ftsZ2p* mutant is consistent with a failure to up-regulate the expression of *ftsZ*, and this up-regulation is required for developmentally-associated cell division, similarly to what has been observed in *S. coelicolor* and *S. griseus* [11, 50].

Null mutants for core divisome genes

In order to clarify the roles of some of the conserved core divisome proteins for *S. venezuelae*, unmarked in-frame null mutants for *ftsQ* (strain DU629), *divIC* (strain DU613), *ftsL* (strain

DU520), *ftsW* (strain DU521) and *ftsI* (strain DU679) were isolated (Fig. 1a). These genes are broadly conserved among bacteria and their products are membrane proteins required for coordinating the cytoplasmic Z ring with the peptidoglycan synthesis machinery [19, 25]. In other bacteria, FtsQ, FtsL and DivIC form a subcomplex that is recruited to the divisome. A 1 MDa complex containing those proteins, along with FtsZ, has been identified for *E. coli* [51]. Likewise, FtsI and FtsW form a subcomplex involved in septal peptidoglycan synthesis as a transpeptidase and transglycosylase, respectively [27]. While it has not been demonstrated directly for *Streptomyces*, it is reasonable to expect that the protein subcomplexes are conserved.

Since most of the core divisome genes are part of the complex *dcw* gene cluster (Fig. 1a) and are likely co-transcribed with other cell wall biosynthetic genes, unmarked in-frame deletions were generated to avoid polar effects on downstream genes. The mutants were readily isolated and showed consistent macroscopic and microscopic phenotypes that were strikingly similar to one another on MYM agar, but were distinct from the *ftsZ*-null and *ftsZ2p* mutants. In contrast to the *ftsZ*-null mutant, plating efficiency was unaffected in these mutants (Fig. S1), suggesting that vegetative cross-wall formation was not severely impaired. Likewise, aerial mycelium development was essentially unaffected, however, aerial hyphae were not efficiently converted into chains of spores. By 48 hrs of incubation on solid medium, the majority of aerial mycelium had been converted into spores for the wild type. For the *ftsQ*, *ftsL*, *divIC*, *ftsW* and *ftsI* null mutants, a mixture of spores, hyphal fragments and frequent lysed compartments were observed (Figs. 1b and S5). Aerial hyphae often contained frequent and regularly-spaced constrictions, reminiscent of sporulation septa (Fig. 1b). Some separated spores were produced and fragments of varying lengths were also observed for each of these mutants, showing that the products of these genes are not absolutely required for cell division for *S. venezuelae* (Figs. 1b and S5). Each mutation was genetically complemented using site-specific integration plasmids with inserts shown in Figure 1a. The complemented strains sporulate similar to the wild type parent indicating that the phenotypes were associated with the introduced null mutations (Figs. 1b and S1). Combining *ftsQ*, *divIC* and *ftsL* mutations as either double mutants or as a triple mutant did not have a synthetic effect on the observed phenotypes, as judged by phase-contrast microscopy (Fig. 2), suggesting that the loss of all the parts of the putative subcomplex formed by their gene products is no more deleterious than the loss of any one component. This result is consistent with the interpretation that missing any one component must inactivate the remainder of the tripartite

complex. In addition, a double mutant lacking both *ftsW* and *ftsI* was also constructed and the phenotype was indistinguishable from the individual *ftsW* and *ftsI* mutants (Fig. 2), suggesting that the loss of both parts of the putative subcomplex formed by their gene products is no more deleterious than the loss of either one component. Finally, deleting both adjacent *ftsL* and *ftsI* genes together resulted in a mutant with a similar phenotype to an *ftsI* single mutant (Fig. 2), indicating that removal of parts of both putative divisome subcomplexes is no more deleterious than the loss of one part. The similarity of the core mutant phenotypes and lack of synergism when combining divisome mutations seems to support a model where there is no apparent hierarchy of assembly of the core divisome components in *S. venezuelae*. Further experimentation will be needed to clarify the situation and define each contribution.

Spores could be isolated from the aerial mycelium of surface-grown cultures despite the fact that development-associated division was impaired for core divisome single mutants with a reduction in the number of spores produced relative to the wild type. In order to quantify the severity of reduction in sporulation-associated division in these core divisome mutants, measurements were made of mature spores and hyphal fragments harvested in a typical fashion from agar plates after 4 days incubation. For the wild type, the material harvested consisted almost entirely of spores with an average length of 1.00 (±0.23) μm (Fig. S6). In contrast, the average lengths of the spores and hyphal fragments for the *ftsQ*, *divIC* and *ftsL* mutants were similar at 2.13 (±1.76) μm, 2.75 (±2.67) μm and 2.49 (±3.92) μm, respectively, suggesting that in aerial hyphae when development-associated division resulting in cell separation occurred, every other to every third septum was formed with cell separation in some aerial hyphae. In contrast, the average spore-type compartment lengths were greater for the *ftsW* and *ftsI* mutants, 7.18 (±8.32) μm and 5.73 (±6.00) μm, respectively (Fig. S6), suggesting that in some hyphae with development-associated division leading to cell separation, every sixth to seventh septum may have been completed all the way to detachment of cells.

Phase-contrast microscopy showed that the divisome mutants were capable of division leading to cell separation, but did not provide detail on the septum morphology when division failed. Of the five isolated single mutants, *ftsL* and *ftsI* single mutants were selected for observation by electron microscopy as representative examples of mutants affecting the putative FtsQ-DivIC-FtsL complex and the FtsW-FtsI complex. TEM analysis for an *ftsL*-null mutant indicated that the

evenly-spaced constrictions in aerial hyphae observed by light microscopy represented complete invaginations with very thick peptidoglycan (Fig. 1c), while *ftsI*-null mutants produced more normal looking septa (Fig. 1c), but at a lower frequency.

While extremely rare in the wild type strain, branching within nascent spore chains was commonly observed for the *ftsQ*, *divIC*, *ftsL*, *ftsW* and *ftsI* mutants. Both the cell division defect and the observed branching phenotype in aerial hyphae were rescued in genetic complementation studies, confirming that the phenotypes are associated with the deletion of these genes and not the result of unlinked mutations (Fig. 1b).

Core divisome proteins are not absolutely required for genome segregation in *S. venezuelae*

To further characterize the cell division and sporulation defects in *ftsZ*, *ftsZ2p*, *ftsQ*, *ftsL*, *divIC*, *ftsW* and *ftsI* mutants of *S. venezuelae*, the cell wall was stained using WGA-FITC and nucleoids were stained by propidium iodide (Figs. 3 and S7). Cell wall staining confirmed that hyphae of the *ftsZ*-null mutant had no signs of invagination, vegetative cross walls or sporulation septa. In addition, there was no evidence of DNA condensation either (Fig. 3). In contrast, partial nucleoid condensation and segregation was observed for the *ftsZ2p* developmental promoter mutant (Fig. 3).

Consistent with observations from phase-contrast and TEM microscopy, *ftsQ*, *ftsL*, *divIC*, *ftsW* and *ftsI* mutants showed very similar patterns of cell wall and DNA staining (Figs. 3 and S7). In aerial hyphae with constrictions visible by light microscopy, ladders of nascent septal wall material could be seen. However, these ladders were often not as regular as the evenly-spaced ones seen for the wild type. DNA segregation was not grossly affected by the loss of any of these division genes, but often was less uniform than for the wild type. Overall, under the laboratory conditions that we tested, we conclude that *S. venezuelae* is able to lay down cell division septa and segregate their genomes even in the absence of the core divisome genes *ftsQ*, *ftsL*, *divIC*, *ftsW* or *ftsI*. Future avenues of research will be necessary to understand why these genes are conserved, yet their products are not essential for septum formation for this filamentous bacterium.

Assembly of FtsZ into ladder-like arrays of Z rings in sporogenic hyphae does not require the core divisome genes *ftsQ*, *ftsL*, *divIC*, and *ftsW*

Next, using a subset of the mutants, we investigated to what extent the core divisome mutations affected the localization and dynamics of FtsZ rings in *S. venezuelae*. In order to do this, *ftsZ-ypet* (pKF351) was introduced into the ΦBT1 *att* site of *ftsQ*, *ftsL*, *divIC*, and *ftsW* mutants, as well as the wild type strain, leading to production of FtsZ fused to the yellow fluorescent protein YPet in addition to the native FtsZ. In vegetative hyphae sampled from standard liquid medium cultures at different stages along the growth curve, we observed an apparently normal distribution of Z rings in vegetative hyphae (not shown, but see also microfluidics data below). Further, sporulating hyphae with multiple, closely and regularly-spaced Z rings were observed in both the wild type strain and the *ftsQ*, *ftsL*, *divIC*, and *ftsW* mutants (Fig. 4), albeit examples of sporulating hyphae were observed at a lower frequency in the mutants than in the wild type.

In order to observe more clearly how mutations in core divisome genes affect FtsZ dynamics and Z-ring formation, we used microfluidics-based fluorescence live cell imaging, as described previously [35, 47]. Representative micrographs of FtsZ ladders formed in the wild type and *ftsQ* and *ftsW* mutants under these conditions are shown in Fig. 5. Time lapse images were also acquired to visualize the FtsZ dynamics. In the wild type, during vegetative stage, typical Z rings are observed that are highly dynamic as shown by their movement along the hyphae before they stabilize at fixed positions and then increase in fluorescence intensity (Movie S1). Presumably, these observed intense Z rings mark sites of vegetative cross-wall formation. A very similar pattern was seen for formation of Z rings in early growth timepoints for vegetative hyphae of the *ftsQ* and *ftsW* mutants (Movies S2 and S3, respectively). FtsZ dynamics were also visualized during the sporulation stage for the wild type parent, where examples of the assembly of evenly-spaced Z rings in ladder-like patterns could be seen in sporogenic hyphae (Movie S1, >10 hours of growth in this sample). Intriguingly, similar development-associated FtsZ dynamics were observed in the mutants for *ftsQ* (Movie S2) and *ftsW* (Movie S3) and the assembly of evenly-spaced FtsZ ladders occurred. Closer inspection of the stability FtsZ ladder persistence was accomplished by constructing a montage from timepoint images for the wild type parent and the *ftsQ* and *ftsW* mutants (Fig. 6). The FtsZ ladders persist for approximately two hours for the wild type, but the ladders do not show the same dynamics for the mutants. Certain FtsZ rings are lost over time in

the mutants, with the rungs of FtsZ ladders in the *ftsW* mutant being the least stable. These relative FtsZ ladder stabilities correlate with the average lengths of mature spores that can be harvested from surface grown cultures (Fig. S6), with the spores for *ftsQ* and *ftsW* mutants being approximately 2X and 7X the length of those produced by the wild type.

Physiological relevance of cumulative results

Overall, the results clearly show that the products of the divisome genes *ftsQ*, *ftsL*, *divIC*, and *ftsW* are not required for Z-ring assembly, for the single Z rings that are formed in vegetative hyphae (normally leading to hyphal cross-walls in the wild type), and in sporogenic hyphae, where ladders of regularly spaced Z rings are typically formed as part of sporulation septation. . In some instances, Z-ring formation appeared essentially normal in the *ftsQ*, *ftsL*, *divIC*, and *ftsW* mutants. The results are consistent with the previously observed ability of corresponding mutants in *S. coelicolor* to form cross-walls and septa, at least under certain conditions [28-31]. It has been speculated previously that *ftsW* may be required for Z-ring assembly, and may provide a membrane attachment for FtsZ in both *S. coelicolor* and *Mycobacterium smegmatis* [31, 52]. Our results presented here for *S. venezuelae* show that *ftsW* is not required for Z-ring formation.

The fact that core cell division proteins FtsQ, FtsL, DivIC, FtsW and FtsI are not strictly required for cell division in *Streptomyces* spp. gives rise to interesting questions to be investigated in future studies. For example, how is it possible to carry out cell division in the absence of the FtsQ-FtsL-DivIC complex? Either the divisome in *Streptomyces* spp. can be stable and functional without these proteins, or there are other proteins that can replace or reinforce these core divisome proteins. In the latter case, such proteins would be pertinent to identify. Interestingly, co-immunoprecipitation experiments identified 63 FtsQ-interacting proteins for *Mycobacterium tuberculosis* and may point to homologs for further investigation [53].

Similarly, how can cell division occur in the absence of FtsW and its cognate transpeptidase FtsI? The transpeptidase of FtsI has been shown to be nonessential for some other gram-positive bacteria, although the protein is still physically required [54-56]. In the absence of FtsI, perhaps FtsW functions with one or more of the many PBPs encoded for *S. venezuelae*. FtsI transpeptidase activity can be supplied by other PBPs in *B. subtilis* [56]. FtsW co-purifies with two different PBPs

in a potential trimeric complex in *E. coli* [57]. FtsW has recently been identified as a peptidoglycan transglycosylase (essentially a peptidoglycan polymerase) [27], in similarity to related RodA SEDS proteins [58-60]. These are essential activities for formation of a cell division septum, and the results presented here suggests that another peptidoglycan polymerase likely is recruited to Z rings at division sites in order for the *S. venezuelae ftsW* mutant to form septa. As one possibility, perhaps transglycosylase activity can be provided by an autonomous bifunctional class A PBP and not by a SEDS protein. In support of that notion, evidence for intimate participation of bifunctional PBPs in septum peptidoglycan synthesis has been accumulating [61]. Recent evidence suggests that pneumococcal peptidoglycan is synthesized, in part, by bifunctional PBPs [62]. As another possibility, one of the other three SEDS proteins encoded by streptomycete genomes [29, 31] may be active either at the same time as FtsW and/or induced in the absence. It will be interesting to see which protein(s) functions in a *ftsW* mutant and how it would be recruited to the divisome. Of final note, we also have constructed strains individually expressing EFGP fusions to each protein of the FtsQ-FtsL-DivIC or FtsI-FtsW complexes and the fluorescent localization signals are not strong enough to publish (data not shown). Potentially, the weak fluorescence signal is indicative of a low intracellular concentration. Again, future work will have to be done to learn if small amounts of the proteins are needed for normal function, if another protein can substitute, or if multiple SEDS-PBP pairs work simultaneously during sporulation septum formation.

SUMMARY AND CONCLUSIONS

In this study, we have established the contributions of known central cell division proteins in the coordinated process of sporulation septation in *S. venezuelae*. Knowing the null phenotypes for mutants lacking known players in cell division will be essential for future studies as we continue to peel back the novel lineage-specific layers of controls evolved to govern the concerted development-associated control of essential cell biological processes in streptomycetes.

In this study, we have taken advantage of the benefits of *S. venezuelae* to visualize the synchronous events being orchestrated within sporogenic hyphae by live-cell time-lapse microscopy because this species undergoes differentiation under submerged growth conditions. The data show that ladder-like assemblages of evenly-spaced FtsZ rings typically form in all of the characterized core divisome mutants. Thus, the tested divisome components are not required for that early coordinated event. However, once formed the Z-rings appear to be unstable and a number of rings

prematurely disband. The loss of coordination results in irregular spacing between completed septa and irregular spore size, as seen in the divisome mutants.

Evidence has accumulated for subcomplex formation of FtsQ-FtsL-DivIC and FtsW-FtsI before participation in the divisome. For *S. venezuelae*, combining mutations of genes encoding these components do not result in synthetic phenotypes. The result is consistent with the interpretation that the loss of any one component disrupts the function of the subcomplex. While the subcomplexes are not absolutely required, they do contribute to the stability of the synchronous tandem arrays of divisome complexes as visualized by FtsZ-YPet. Recently, analysis of bacterial dynamins DynA and DynB for *S. venezuelae* showed that they interact with the division machinery [18], contribute to Z-ring stability and mutants encoding those proteins have somewhat similar phenotypes as the divisome mutants reported here. Future work will be needed to understand how these components interact and are regulated to synchronously coordinate sporulation septum formation.

ACKNOWLEDGEMENTS

SC and JRM thank John Stolz for help with electron microscopy and John Pollock and Philip Auron for help with fluorescence microscopy.

Funding information

Support for this work was provided by National Institutes of Health grant GM096268 (JRM), Swedish Research Council grant 621-2010-4463 (KF), Crafoord Foundation grant 20140962 (KF) and Wenner-Gren guest rersearcher grant (KF and JRM); stipend support was provided by the Bayer School of Natural and Environmental Sciences, Duquesne University (SC); BCS was supported by the Sven och Lilly Lawskis fond för naturvetenskaplig forskning, Stiftelsen Jörgen Lindströms stipendiefond, and the Royal Physiographic Society of Lund.

Conflicts of interest

The authors declare no conflict of interests.

539 **REFERENCES**

540 1. **Hopwood DA.** Forty years of genetics with *Streptomyces*: from *in vivo* through
541 *in vitro* to *in silico*. *Microbiology*. 1999;145:2183-202. Doi: 10.1099/00221287-145-9-
542 2183
543 2. **Barka EA, Vatsa P, Sanchez L, Gaveau-Vaillant N, Jacquard C, Meier-**
544 **Kolthoff JP, et al.** Taxonomy, physiology, and natural products of Actinobacteria.
545 *Microbiol Mol Biol Rev*. 2016;80:1-43. Doi: 10.1128/MMBR.00019-15
546 3. **Bush MJ, Tschowri N, Schlimpert S, Flärdh K, Buttner MJ.** c-di-GMP
547 signalling and the regulation of developmental transitions in streptomycetes. *Nat Rev*
548 *Microbiol*. 2015;13:749-60. Doi: 10.1038/nrmicro3546
549 4. **McCormick JR, Flärdh K.** Signals and regulators that govern *Streptomyces*
550 development. *FEMS Microbiol Rev*. 2012;36:206-31. Doi:
551 5. **Elliot MA, Flärdh K.** Streptomycete spores. eLS. Chichester: John Wiley &
552 Sons Ltd; 2020. Doi: 10.1002/9780470015902.a0000308.pub3
553 6. **Jakimowicz D, van Wezel GP.** Cell division and DNA segregation in
554 *Streptomyces*: how to build a septum in the middle of nowhere? *Mol Microbiol*.
555 2012;85:393-404. Doi: 10.1111/j.1365-2958.2012.08107.x
556 7. **McCormick JR.** Cell division is dispensable but not irrelevant in *Streptomyces*.
557 *Curr Opin Microbiol*. 2009;12:689-98. Doi:
558 8. **McCormick JR, Su EP, Driks A, Losick R.** Growth and viability of
559 *Streptomyces coelicolor* mutant for the cell division gene *ftsZ*. *Mol Microbiol*.
560 1994;14:243-54. Doi:
561 9. **Santos-Beneit F, Roberts DM, Cantlay S, McCormick JR, Errington J.**
562 A mechanism for FtsZ-independent proliferation in *Streptomyces*. *Nat Commun*.
563 2017;8:1378. Doi: 10.1038/s41467-017-01596-z
564 10. **Wildermuth H, Hopwood DA.** Septation during sporulation in *Streptomyces*
565 *coelicolor*. *J Gen Microbiol*. 1970;60:57-9. Doi:
566 11. **Flärdh K, Leibovitz E, Buttner MJ, Chater KF.** Generation of a non-
567 sporulating strain of *Streptomyces coelicolor* A3(2) by the manipulation of a
568 developmentally controlled *ftsZ* promoter. *Mol Microbiol*. 2000;38:737-49. Doi:
569 12. **den Hengst CD, Tran NT, Bibb MJ, Chandra G, Leskiw BK, Buttner**
570 **MJ.** Genes essential for morphological development and antibiotic production in
571 *Streptomyces coelicolor* are targets of BldD during vegetative growth. *Mol Microbiol*.
572 2010;78:361-79. Doi: 10.1111/j.1365-2958.2010.07338.x
573 13. **Tschowri N, Schumacher MA, Schlimpert S, Chinnam NB, Findlay KC,**
574 **Brennan RG, et al.** Tetrameric c-di-GMP mediates effective transcription factor
575 dimerization to control *Streptomyces* development. *Cell*. 2014;158:1136-47. Doi:
576 10.1016/j.cell.2014.07.022
577 14. **Bush MJ, Bibb MJ, Chandra G, Findlay KC, Buttner MJ.** Genes required
578 for aerial growth, cell division, and chromosome segregation are targets of WhiA before
579 sporulation in *Streptomyces venezuelae*. *MBio*. 2013;4:e00684-13. Doi:
580 10.1128/mBio.00684-13
581 15. **Bush MJ, Chandra G, Bibb MJ, Findlay KC, Buttner MJ.** Genome-wide
582 chromatin immunoprecipitation sequencing analysis shows that WhiB is a transcription
583 factor that cocontrols its regulon with WhiA to initiate developmental cell division in
584 *Streptomyces*. *MBio*. 2016;7:e00523-16. Doi: 10.1128/mBio.00523-16

585 16. **Al-Bassam MM, Bibb MJ, Bush MJ, Chandra G, Buttner MJ.** Response
586 regulator heterodimer formation controls a key stage in *Streptomyces* development.
587 *PLoS Genet*. 2014;10:e1004554. Doi: 10.1371/journal.pgen.1004554
588 17. **Willemse J, Borst JW, de Waal E, Bisseling T, van Wezel GP.** Positive
589 control of cell division: FtsZ is recruited by SsgB during sporulation of *Streptomyces*.
590 *Genes Dev*. 2011;25:89-99. Doi:
591 18. **Schlimpert S, Wasserstrom S, Chandra G, Bibb MJ, Findlay KC,**
592 **Flärdh K, et al.** Two dynamin-like proteins stabilize FtsZ rings during *Streptomyces*
593 sporulation. *Proc Natl Acad Sci USA*. 2017;114:E6176-E83. Doi:
594 10.1073/pnas.1704612114
595 19. **Du S, Lutkenhaus J.** Assembly and activation of the *Escherichia coli* divisome.
596 *Mol Microbiol*. 2017;105:177-87. Doi: 10.1111/mmi.13696
597 20. **Haeusser DP, Margolin W.** Splitsville: structural and functional insights into
598 the dynamic bacterial Z ring. *Nat Rev Microbiol*. 2016;14:305-19. Doi:
599 10.1038/nrmicro.2016.26
600 21. **Ortiz C, Natale P, Cueto L, Vicente M.** The keepers of the ring: regulators of
601 FtsZ assembly. *FEMS Microbiol Rev*. 2016;40:57-67. Doi: 10.1093/femsre/fuv040
602 22. **Duman R, Ishikawa S, Celik I, Strahl H, Ogasawara N, Troc P, et al.**
603 Structural and genetic analyses reveal the protein SepF as a new membrane anchor for
604 the Z ring. *Proc Natl Acad Sci USA*. 2013;110:E4601-E10. Doi:
605 10.1073/pnas.1313978110
606 23. **Zhang L, Willemse J, Claessen D, van Wezel GP.** SepG coordinates
607 sporulation-specific cell division and nucleoid organization in *Streptomyces coelicolor*.
608 *Open Biol*. 2016;6:150164. Doi: 10.1098/rsob.150164
609 24. **Del Sol R, Mullins JG, Grantcharova N, Flärdh K, Dyson P.** Influence of
610 CrgA on assembly of the cell division protein FtsZ during development of *Streptomyces*
611 *coelicolor*. *J Bacteriol*. 2006;188:1540-50. Doi:
612 25. **Buddelmeijer N, Beckwith J.** A complex of the *Escherichia coli* cell division
613 proteins FtsL, FtsB and FtsQ forms independently of its localization to the septal region.
614 *Mol Microbiol*. 2004;52:1315-27. Doi: 10.1111/j.1365-2958.2004.04044.x
615 26. **Boes A, Olatunji S, Breukink E, Terrak M.** Regulation of the peptidoglycan
616 polymerase activity of PBP1b by antagonist actions of the core divisome proteins FtsBLQ
617 and FtsN. *mBio*. 2019;10:e01912-18. Doi: 10.1128/mBio.01912-18
618 27. **Taguchi A, Welsh MA, Marmont LS, Lee W, Sjodt M, Kruse AC, et al.**
619 FtsW is a peptidoglycan polymerase that is functional only in complex with its cognate
620 penicillin-binding protein. *Nat Microbiol*. 2019;4:587-94. Doi: 10.1038/s41564-018-
621 0345-x
622 28. **Bennett JA, Aimino RM, McCormick JR.** *Streptomyces coelicolor* genes
623 *ftsL* and *divIC* play a role in cell division but are dispensable for colony formation. *J*
624 *Bacteriol*. 2007;189:8982-92. Doi:
625 29. **Bennett JA, Yarnall J, Cadwallader AB, Kuennen R, Bidey P,**
626 **Stadelmaier B, et al.** Medium-dependent phenotypes of *Streptomyces coelicolor* with
627 mutations in *ftsI* or *ftsW*. *J Bacteriol*. 2009;191:661-4. Doi:
628 30. **McCormick JR, Losick R.** Cell division gene *ftsQ* is required for efficient
629 sporulation but not growth and viability in *Streptomyces coelicolor* A3(2). *J Bacteriol*.
630 1996;178:5295-301. Doi:

631 31. **Mistry BV, Del Sol R, Wright C, Findlay K, Dyson P.** FtsW is a
632 dispensable cell division protein required for Z-ring stabilization during sporulation
633 septation in *Streptomyces coelicolor*. *J Bacteriol*. 2008;190:5555-66. Doi:
634 10.1128/JB.00398-08
635 32. **Ausmees N, Wahlstedt H, Bagchi S, Elliot MA, Buttner MJ, Flardh K.**
636 SmeA, a small membrane protein with multiple functions in *Streptomyces* sporulation
637 including targeting of a SpoIIIE/FtsK-like protein to cell division septa. *Mol Microbiol*.
638 2007;65:1458-73. Doi: 10.1111/j.1365-2958.2007.05877.x
639 33. **Dedrick RM, Wildschutte H, McCormick JR.** Genetic interactions of *smc*,
640 *ftsK*, and *parB* genes in *Streptomyces coelicolor* and their developmental genome
641 segregation phenotypes. *J Bacteriol*. 2009;191:320-32. Doi:
642 34. **Wang L, Yu Y, He X, Zhou X, Deng Z, Chater KF, et al.** Role of an FtsK-
643 like protein in genetic stability in *Streptomyces coelicolor* A3(2). *J Bacteriol*.
644 2007;189:2310-8. Doi:
645 35. **Schlimpert S, Flärdh K, Buttner M.** Fluorescence time-lapse imaging of the
646 complete *S. venezuelae* life cycle using a microfluidic device. *J Vis Exp*. 2016:e53863.
647 Doi: 10.3791/53863
648 36. **Stuttard C.** Temperate phages of *Streptomyces venezuelae*: lysogeny and
649 specificity shown by phages SV1 and SV2. *Microbiology*. 1982;128:115-21. Doi:
650 37. **Bibb MJ, Domonkos A, Chandra G, Buttner MJ.** Expression of the chaplin
651 and rodlin hydrophobic sheath proteins in *Streptomyces venezuelae* is controlled by
652 sigma(BldN) and a cognate anti-sigma factor, RsbN. *Mol Microbiol*. 2012;84:1033-49.
653 Doi: 10.1111/j.1365-2958.2012.08070.x
654 38. **Kieser T, Bibb MJ, Buttner MJ, Chater KF, Hopwood DA.** Practical
655 Streptomyces Genetics. Norwich, UK: The John Innes Foundation; 2000.
656 39. **Sambrook J, Fritsch EF, Maniatis T.** Molecular Cloning: A Laboratory
657 Manual. Second ed. Cold Spring Harbor, NY: Cold Spring Harbor Laboratory Press;
658 1989.
659 40. **Datsenko KA, Wanner BL.** One-step inactivation of chromosomal genes in
660 *Escherichia coli* K-12 using PCR products. *Proc Natl Acad Sci U S A*. 2000;97:6640-5.
661 Doi: 10.1073/pnas.120163297
662 41. **Gust B, Challis GL, Fowler K, Kieser T, Chater KF.** PCR-targeted
663 *Streptomyces* gene replacement identifies a protein domain needed for biosynthesis of
664 the sesquiterpene soil odor geosmin. *Proc Natl Acad Sci U S A*. 2003;100:1541-6. Doi:
665 10.1073/pnas.0337542100
666 42. **Datsenko KA, Wanner BW.** One-step inactivation of chromosomal genes in
667 *Escherichia coli* K-12 using PCR products. *Proc Natl Acad Sci USA*. 2000;97:6640-5.
668 Doi: 10.1073/pnas.120163297
669 43. **Gust B, Challis GL, Fowler K, Kieser T, Chater KF.** PCR-targeted
670 *Streptomyces* gene replacement identifies a protein domain needed for biosynthesis of
671 the sesquiterpene soil odor geosmin. *Proc Natl Acad Sci USA*. 2003;100:1541-6. Doi:
672 10.1073/pnas.0337542100
673 44. **Cherepanov PP, Wackernagel W.** Gene disruption in *Escherichia coli:* TcR
674 and KmR cassettes with the option of Flp-catalyzed excision of the antibiotic-resistance
675 determinant. *Gene*. 1995;158:9-14. Doi: 10.1016/0378-1119(95)00193-a

676 45. **Gregory MA, Till R, Smith MC.** Integration site for *Streptomyces* phage
677 phiBT1 and development of site-specific integrating vectors. *J Bacteriol*.
678 2003;185:5320-3. Doi: 10.1128/jb.185.17.5320-5323.2003
679 46. **Donczew M, Mackiewicz P, Wrobel A, Flärdh K, Zakrzewska-**
680 **Czerwinska J, Jakimowicz D.** ParA and ParB coordinate chromosome segregation
681 with cell elongation and division during *Streptomyces* sporulation. *Open Biol*.
682 2016;6:150263. Doi: 10.1098/rsob.150263
683 47. **Sen BC, Wasserstrom S, Findlay KC, Söderholm N, Sandblad L, von**
684 **Wachenfeldt C, et al.** Specific amino acid substitutions in β strand S2 of FtsZ cause
685 spiraling septation and impair assembly cooperativity in *Streptomyces*. *Mol Microbiol*.
686 2019;112:184-98. Doi: 10.1111/mmi.14262
687 48. **Schindelin J, Arganda-Carreras I, Frise E, Kaynig V, Longair M,**
688 **Pietzsch T, et al.** Fiji: an open-source platform for biological-image analysis. *Nat*
689 *Methods*. 2012;9:676-82. Doi: 10.1038/nmeth.2019
690 49. **Bush MJ, Chandra G, Al-Bassam MM, Findlay KC, Buttner MJ.** BldC
691 delays entry into development to produce a sustained period of vegetative growth in
692 *Streptomyces venezuelae*. *MBio*. 2019;10:e02812-18. Doi: 10.1128/mBio.02812-18
693 50. **Kwak J, Dharmatilake AJ, Jiang H, Kendrick KE.** Differential regulation
694 of *ftsZ* transcription during septation of *Streptomyces griseus*. *J Bacteriol*.
695 2001;183:5092-101. Doi:
696 51. **Trip EN, Scheffers DJ.** A 1 MDa protein complex containing critical
697 components of the *Escherichia coli* divisome. *Sci Rep*. 2015;5:18190. Doi:
698 10.1038/srep18190
699 52. **Datta P, Dasgupta A, Bhakta S, Basu J.** Interaction between FtsZ and FtsW
700 of *Mycobacterium tuberculosis*. *J Biol Chem*. 2002;277:24983-7. Doi:
701 10.1074/jbc.M203847200
702 53. **Wu KJ, Zhang J, Baranowski C, Leung V, Rego EH, Morita YS, et al.**
703 Characterization of conserved and novel septal factors in *Mycobacterium smegmatis*. *J*
704 *Bacteriol*. 2018;200:e00649-17. Doi: 10.1128/JB.00649-17
705 54. **Morales Angeles D, Liu Y, Hartman AM, Borisova M, Borges AD, de**
706 **Kok N, et al.** Pentapeptide-rich peptidoglycan at the *Bacillus subtilis* cell-division site.
707 *Mol Microbiol*. 2017;104:319-33. Doi: 10.1111/mmi.13629
708 55. **Peters K, Schweizer I, Beilharz K, Stahlmann C, Veening JW,**
709 **Hakenbeck R, et al.** *Streptococcus pneumoniae* PBP2x mid-cell localization requires
710 the C-terminal PASTA domains and is essential for cell shape maintenance. *Mol*
711 *Microbiol*. 2014;92:733-55. Doi: 10.1111/mmi.12588
712 56. **Sassine J, Xu MZ, Sidiq KR, Emmins R, Errington J, Daniel RA.**
713 Functional redundancy of division specific penicillin-binding proteins in *Bacillus*
714 *subtilis*. *Mol Microbiol*. 2017;106:304-18. Doi: 10.1111/mmi.13765
715 57. **Leclercq S, Derouaux A, Olatunji S, Fraipont C, Egan AJ, Vollmer W,**
716 **et al.** Interplay between Penicillin-binding proteins and SEDS proteins promotes
717 bacterial cell wall synthesis. *Sci Rep*. 2017;7:43306. Doi: 10.1038/srep43306
718 58. **Cho H, Wivagg CN, Kapoor M, Barry Z, Rohs PDA, Suh H, et al.**
719 Bacterial cell wall biogenesis is mediated by SEDS and PBP polymerase families
720 functioning semi-autonomously. *Nat Microbiol*. 2016;1:16172. Doi:
721 10.1038/nmicrobiol.2016.172

722 59. **Emami K, Guyet A, Kawai Y, Devi J, Wu LJ, Allenby N, et al.** RodA as
723 the missing glycosyltransferase in *Bacillus subtilis* and antibiotic discovery for the
724 peptidoglycan polymerase pathway. *Nat Microbiol*. 2017;2:16253. Doi:
725 10.1038/nmicrobiol.2016.253
726 60. **Meeske AJ, Riley EP, Robins WP, Uehara T, Mekalanos JJ, Kahne D,**
727 **et al.** SEDS proteins are a widespread family of bacterial cell wall polymerases. *Nature*.
728 2016;537:634-8. Doi: 10.1038/nature19331
729 61. **Pazos M, Peters K, Casanova M, Palacios P, VanNieuwenhze M,**
730 **Breukink E, et al.** Z-ring membrane anchors associate with cell wall synthases to
731 initiate bacterial cell division. *Nat Commun*. 2018;9:5090. Doi: 10.1038/s41467-018-
732 07559-2
733 62. **Straume D, Piechowiak KW, Olsen S, Stamsas GA, Berg KH, Kjos M,**
734 **et al.** Class A PBPs have a distinct and unique role in the construction of the
735 pneumococcal cell wall. *Proc Natl Acad Sci USA*. 2020;117:6129-38. Doi:
736 10.1073/pnas.1917820117

737

FIGURE LEGENDS

Figure 1. Construction and complementation of *S. venezuelae* strains mutant for core division genes.

(a) A physical map of the *dcw* cluster in *S. venezuelae* and the genetic locus of *divIC*. Maps of two regions of the *S. venezuelae* chromosome are shown that contain genes encoding core proteins of the divisome. In each of the two loci, all genes are in the same orientation as the divisome genes. Regions replaced with an apramycin-resistance cassette or an unmarked in-frame deletion mutation are shown above the maps. DNA fragments used for constructing genetic complementation plasmids are shown below the map. **(b) Phase-contrast microscopy of wild type and mutant phenotypes and mutant phenotypes following genetic complementation.** All images are phase-contrast micrographs of cover slip impressions from cultures grown for 2 days at 30°C on MYM agar. The top row contains wild type *S. venezuelae* strain containing the empty complementation vector on the left (wt). Immediately adjacent are shown seven division mutants containing the empty complementation vector pMS82. In the bottom row are shown the seven division mutants containing a complementing fragment cloned into pMS82 which restores sporulation to wild type levels. Scale bar, 5 μm. **(c) Transmission electron micrographs reveal septation and cell wall defects in the *ftsZ*, *ftsI* and *ftsL* mutants.** Cells were grown for 2 days at 30°C on MYM agar and thin sections were viewed by transmission electron microscopy. Mainly spores were observed for the wild type strain (wt). No examples of vegetative cross-walls and sporulation septa were observed for the *ftsZ*-null mutant. White arrow heads indicate formed unresolved sporulation septa in aerial hyphae for the *ftsL and ftsI* mutants. Scale bar, 500 nm.

Figure 2. Double and triple divisome mutants do not have additive or synergistic division phenotypes.

The strains were grown for two days on MYM agar medium at 30°C. Shown are phase-contrast images from impression coverslips of aerial hyphae for double and triple mutant strains. Aerial hyphae of double and triple mutants frequently contain evenly-spaced constrictions as do the single mutants. The double and triple mutant phenotypes are strikingly similar to the single mutants (Fig. 1b) and do not result in synthetic division phenotypes. Scale bar, 5 µm.

Figure 3. DNA segregation and cell wall phenotypes of *S. venezuelae* division mutants.

Cells were grown for 2 days at 30°C on MYM agar and cover slips were pressed onto confluent lawns. Samples of aerial hyphae were stained for cell wall (green) and DNA (red) and viewed by epifluorescence microscopy. The top row contains corresponding DIC light images. Wild type samples contained mainly spores and spore chains. Examples of aerial hyphae of mutant strains Δ*ftsZ*, *ftsZ*Δ*2p*, Δ*ftsL* and Δ*ftsI* are shown. Scale bar, 5 µm.

Figure 4. Z-ring assembly in sporogenic hypha of *S. venezuelae* divisome mutants.

Batch cultures were grown in a standard fashion in liquid MYM at 30ºC and samples were fixed by formaldehyde treatment before cells were mounted for microscopy. Representative micrographs of sporulating hyphae with FtsZ ladders are shown, visualized using YPet-tagged FtsZ. Shown are the wild type control strain and the indicated divisome mutants into which plasmid pKF351[P_{ftsZ}-*ftsZ-ypet*] had been introduced. Scale bars, 2 µm.

Figure 5. Live-cell imaging of Z-ring assembly in sporogenic hypha of *S. venezuelae* wild type and *ΔftsQ* and *ΔftsW* mutants.

Cultures were grown in MYM at 30ºC using a microfluidic system. Representative micrographs of unfixed sporulating hyphae with FtsZ ladders are shown, visualized using YPet-tagged FtsZ. Shown are the wild type control strain and the indicated divisome mutants into which plasmid pKF351[P_{ftsZ}-*ftsZ-ypet*] had been introduced. Scale bars, 2 µm.

Figure 6. FtsQ and FtsW stabilize Z-rings during sporulation-specific cell division.

Shown is a montage of representative time series documenting FtsZ dynamics during spore formation. Strains were grown in liquid MYM at 30ºC using a microfluidic system. Fluorescence images of FtsZ-YPet signal were obtained from time-lapse microscopy (top) and the corresponding phase-contrast images are also shown (bottom). Shown are montages of the wild type control strain and the indicated divisome mutants into which plasmid pKF351[P_{ftsZ}-*ftsZ-ypet*] has been introduced. Time intervals between images were kept at 20 min. In addition, zero min was considered as the time wherein the shown hypha had undergone arrest of tip extension before sporulation septation began. Scale bars, 2 µm.

(a)

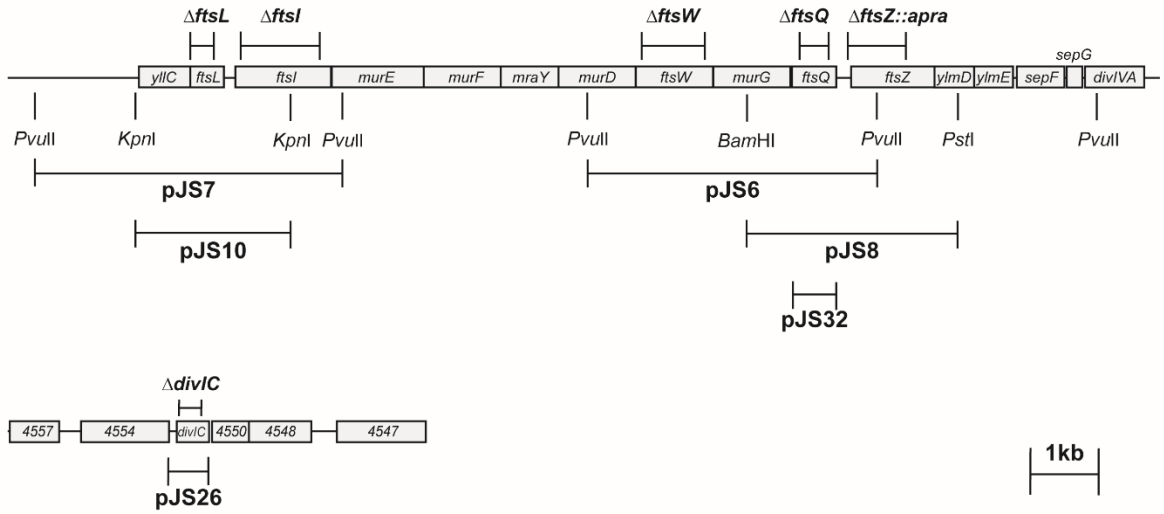
ΔftsL
ΔftsI
ΔftsW
ΔftsQ
ΔftsZ::apra
sepG
yllC
ftsL
ftsI
murE
murF
mraY
murD
ftsW
murG
ftsQ
ftsZ
ylmD
ylmE
sepF
divIVA
PvuII
KpnI
KpnI
PvuII
PvuII
BamHI
PvuII
PstI
PvuII
pJS7
pJS6
pJS10
pJS8
pJS32
ΔdivIC
4557
4554
divIC
4550
4548
4547
pJS26
1kb

(b)

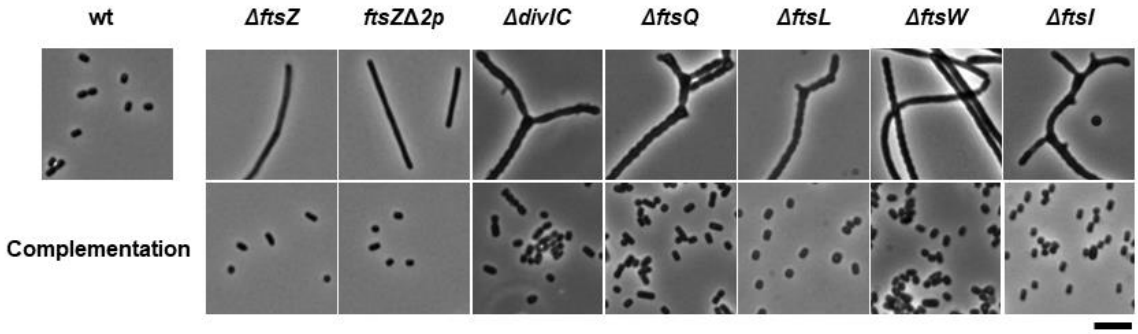
wt
ΔftsZ
ftsZΔ2p
ΔdivIC
ΔftsQ
ΔftsL
ΔftsW
ΔftsI
Complementation

(c)

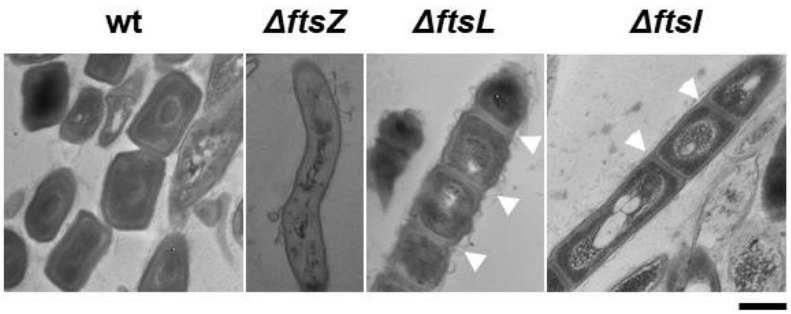
wt
ΔftsZ
ΔftsL
ΔftsI

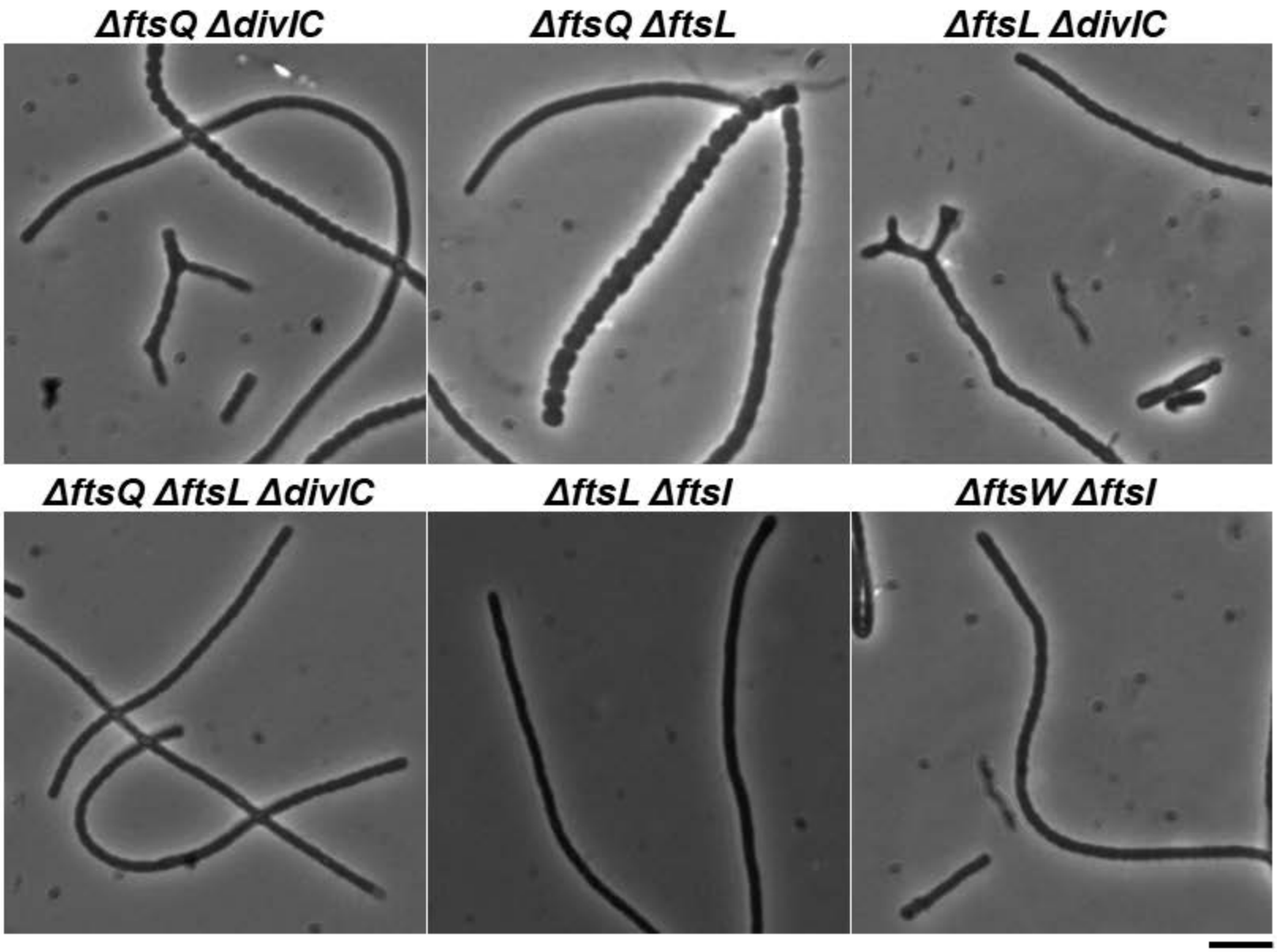
ΔftsQ ΔdivIC
ΔftsQ ΔftsL
ΔftsL ΔdivIC
ΔftsQ ΔftsL ΔdivIC
ΔftsL ΔftsI
ΔftsW ΔftsI

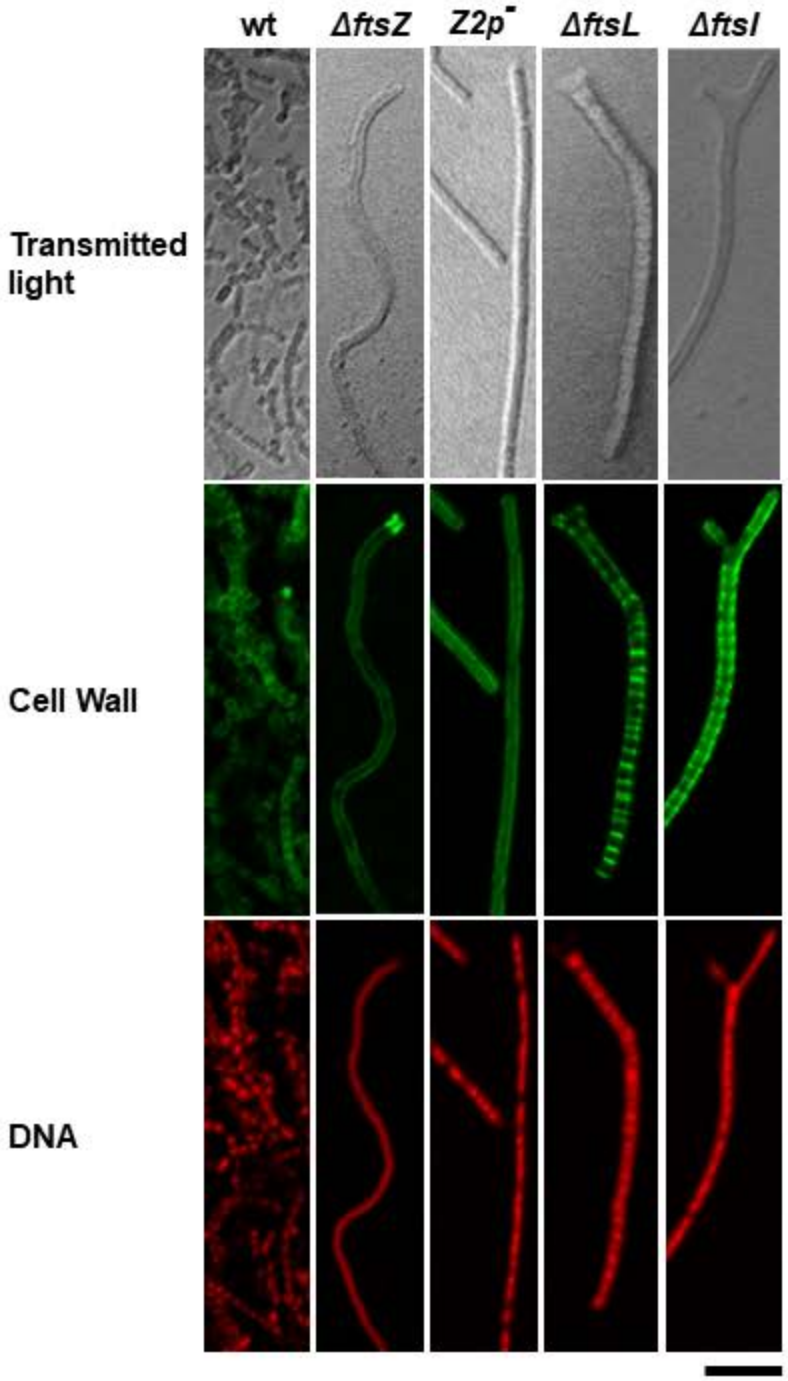
wt
ΔftsZ
Z2p⁻
ΔftsL
ΔftsI
Transmitted light
Cell Wall
DNA

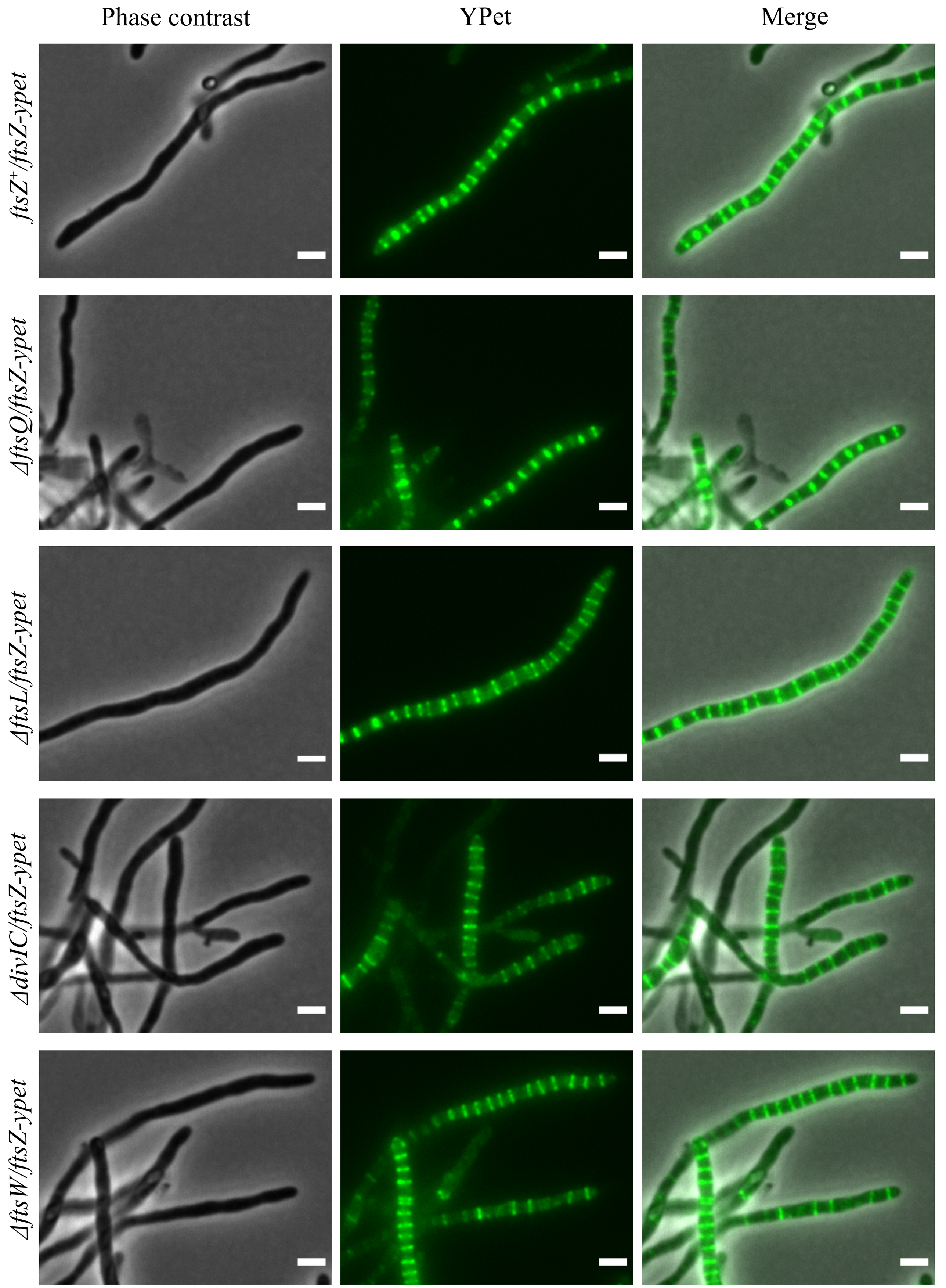
Phase contrast
YPet
Merge
ftsZ+/ftsZ-ypet
ΔftsQ/ftsZ-ypet
ΔftsL/ftsZ-ypet
ΔdivIC/ftsZ-ypet
ΔftsW/ftsZ-ypet

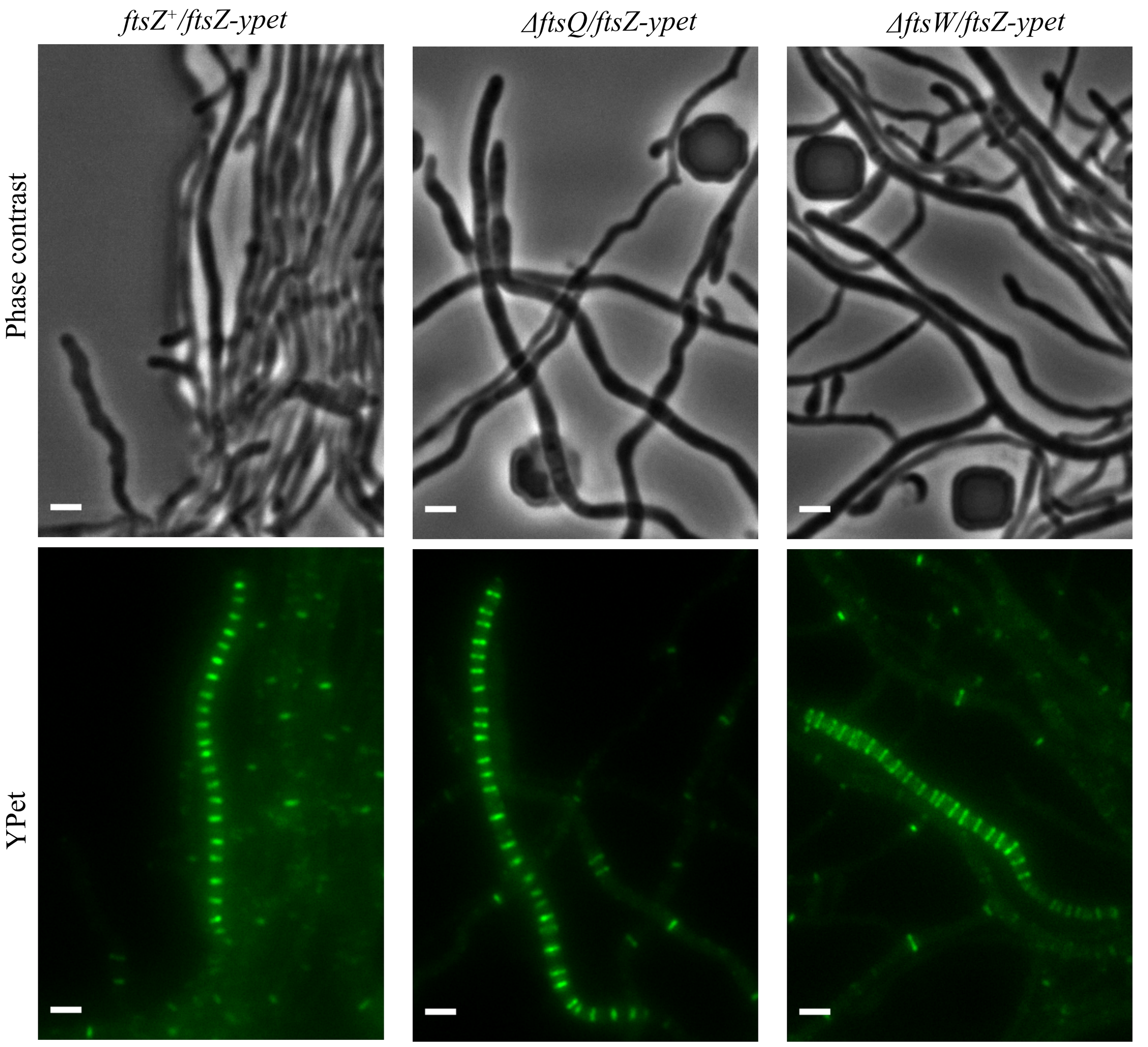
ftsZ+/ftsZ-ypet
ΔftsQ/ftsZ-ypet
ΔftsW/ftsZ-ypet
Phase contrast
YPet

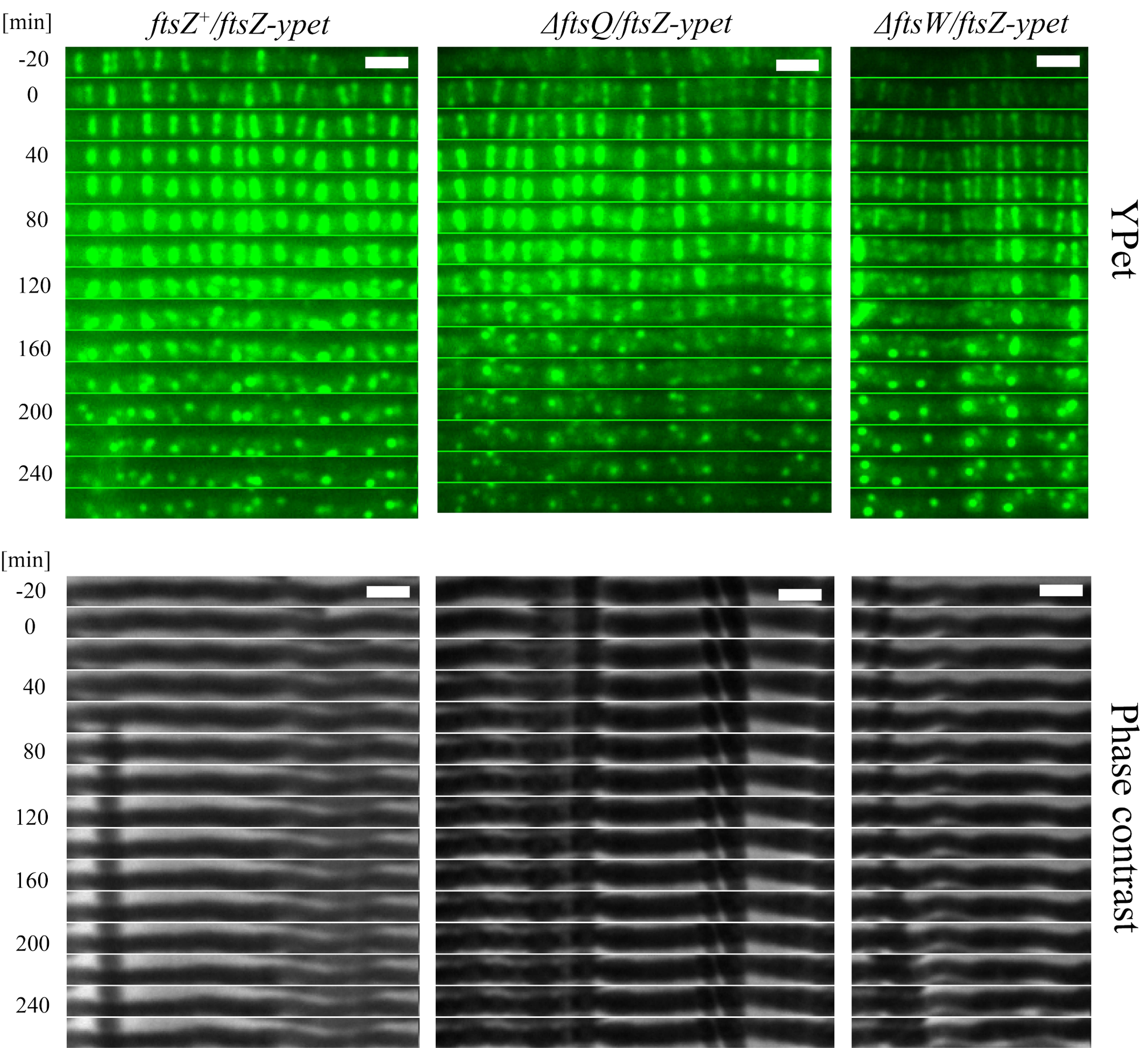
[min]
ftsZ+/ftsZ-ypet
ΔftsQ/ftsZ-ypet
ΔftsW/ftsZ-ypet
-20
0
40
80
120
160
200
240
YPet
[min]
-20
0
40
80
120
160
200
240
Phase contrast

Supplementary material

Influence of core divisome proteins on cell division in *Streptomyces venezuelae* ATCC 10712

Stuart Cantlay[1,#], Beer Chakra Sen[2], Klas Flärdh[2] and Joseph R. McCormick[1,*]

[1] *Department of Biological Sciences, Duquesne University, Pittsburgh, PA 15282, USA*

[2] *Department of Biology, Lund University, 223 62 Lund, Sweden*

[#]*Current address: Department of Biological Sciences, West Liberty University, West Liberty, WV 26074, USA*

**Corresponding author*

Department of Biological Sciences, Duquesne University, Pittsburgh, PA 15282, USA

Tel: (+1) 412 396 4775

Email: mccormick@duq.edu

Table S1. *S. venezuelae* Strains

Strain Genotypes[†]	**ATCC 10712**	**NRRL B-65442**	**Comments**[‡]
attB$_{\Phi BT1}$::pMS82	DU522	DU732	cloning vector integrated by site specific recombination, Hyg^R
attB$_{\Phi BT1}$::pJS26 (*divIC*$^+$)	DU620		*divIC*$^+$ genetic complementation vector integrated *in trans*
attB$_{\Phi BT1}$::pJS7 (*ftsIL*$^+$)	DU528		*ftsIL*$^+$ genetic complementation vector integrated *in trans*
attB$_{\Phi BT1}$::pJS10 (*ftsL*$^+$)	DU538		*ftsL*$^+$ genetic complementation vector integrated *in trans*
attB$_{\Phi BT1}$::pJS32 (*Pdcw-ftsQ*$^+$)	DU626		*ftsQ*$^+$ genetic complementation vector integrated *in trans*
attB$_{\Phi BT1}$::pJS6 (*ftsW*$^+$)	DU524		*ftsW*$^+$ genetic complementation vector integrated *in trans*
attB$_{\Phi BT1}$::pJS8 (*ftsZ*$^+$)	DU534		*ftsZ*$^+$ genetic complementation vector integrated *in trans*
attB$_{\Phi C31}$::pKF280 (*ypet*)	DU576	DU733	*ypet* cloning vector integrated by site specific recombination, Apra^R
attB$_{\Phi C31}$::pKF351 *(ftsZ-ypet)*	DU578	DU724	*ftsZ-ypet* fusion vector integrated *in trans* by site specific recombination
Δ*divIC*::*apra*	DU518	DU519	471 bp deletion of *divIC* including the start and stop codons
Δ*divIC*	DU613		471 bp deletion of *divIC* including the start and stop codons
Δ*divIC attB*$_{\Phi BT1}$::pMS82	DU614		cloning vector integrated by site specific recombination in DU613
Δ*divIC attB*$_{\Phi BT1}$::pJS26 (*divIC*$^+$)	DU615		*divIC*$^+$ genetic complementation vector integrated *in trans* in DU613
Δ*divIC attB*$_{\Phi C31}$::pKF280	DU634		*ypet* cloning vector integrated by site specific recombination DU613
Δ*divIC attB*$_{\Phi C31}$::pKF351 (*ftsZ-ypet*)	DU635		*ftsZ-ypet* fusion vector integrated *in trans* by site specific recombination in DU613
Δ*divIC* Δ*ftsL*	DU592		Mutation in DU613 introduced into DU520
Δ*divIC* Δ*ftsL* Δ*ftsQ*	DU628		Mutation in DU629 introduced into DU592
Δ*divIC* Δ*ftsQ*	DU636		Mutation in DU613 introduced into DU629
Δ*ftsI*::*apra*	DU508	DU509	1,140 bp deletion beginning 60 bp downstream of the *ftsI* start codon
Δ*ftsI*::*frt*	DU679		1,140 bp deletion beginning 60 bp downstream of the *ftsI* start codon with insertion of 81 bp *frt* scar
Δ*ftsI*::*frt attB*$_{\Phi BT1}$::pMS82	DU683		cloning vector integrated by site specific recombination in DU679
Δ*ftsI*::*frt attB*$_{\Phi BT1}$::pJS7 (*ftsIL*$^+$)	DU691		*ftsIL*$^+$ genetic complementation vector integrated *in trans* in DU679
Δ*ftsI*::*frt attB*$_{\Phi C31}$::pKF280	DU681		*ypet* cloning vector integrated by site specific recombination DU679
Δ*ftsI*::*frt attB*$_{\Phi C31}$::pKF351 (*ftsZ-ypet*)	DU680		*ftsZ-ypet* fusion vector integrated *in trans* by site specific recombination in DU679
Δ*ftsIL*::*apra*	DU516	DU517	1,817 bp deletion beginning 5 bp downstream of the *ftsL* start codon through 984 bp downstream of the *ftsI* start codon
Δ*ftsIL*::*apra attB*$_{\Phi BT1}$::pMS82	DU574		cloning vector integrated by site specific recombination in DU516
Δ*ftsIL*::*apra attB*$_{\Phi BT1}$::pJS7 (*ftsIL*$^+$)	DU570		pJS7 integrated at the ΦBT1 attachment site in DU516
Δ*ftsI*::*apra* Δ*ftsW*	DU594		Mutation in DU521 introduced into DU508
Δ*ftsL*::*apra*	DU510	DU511	352 bp deletion beginning 5 bp downstream of the *ftsL* start codon
Δ*ftsL*	DU520		352 bp deletion beginning 5 bp downstream of the *ftsL* start codon
Δ*ftsL attB*$_{\Phi BT1}$::pMS82	DU544		cloning vector integrated by site specific recombination in DU520
Δ*ftsL attB*$_{\Phi BT1}$::pJS10 (*ftsL*$^+$)	DU546		*ftsL*$^+$ genetic complementation vector integrated *in trans* in DU520
Δ*ftsL attB*$_{\Phi C31}$::pKF280	DU588		*ypet* cloning vector integrated by site specific recombination DU520
Δ*ftsL attB*$_{\Phi C31}$::pKF351 (*ftsZ-ypet*)	DU590		*ftsZ-ypet* fusion vector integrated *in trans* by site specific recombination in DU520
Δ*ftsL* Δ*ftsQ*::*apra*	DU622		Mutation in DU520 introduced into DU502
Δ*ftsQ*::*apra*	DU502	DU503	810 bp deletion beginning at the second codon of *ftsQ*
Δ*ftsQ*	DU629		810 bp deletion beginning at the second codon of *ftsQ*
Δ*ftsQ attB*$_{\Phi BT1}$::pMS82	DU630		cloning vector integrated by site specific recombination in DU629

Δ*ftsQ attB*$_{\Phi BT1}$::pJS32 (*Pdcw-ftsQ*$^{+}$)	DU631		*ftsQ*$^{+}$ genetic complementation vector integrated *in trans* in DU629
Δ*ftsQ attB*$_{\Phi C31}$::pKF280	DU632		*ypet* cloning vector integrated by site specific recombination DU629
Δ*ftsQ attB*$_{\Phi C31}$::pKF351 (*ftsZ-ypet*)	DU633		*ftsZ-ypet* fusion vector integrated *in trans* by site specific recombination in DU629
Δ*ftsW*::*apra*	DU512	DU513	1,076 bp deletion beginning 140 bp downstream of the *ftsW* start codon
Δ*ftsW*	DU521		1,076 bp deletion beginning 140 bp downstream of the *ftsW* start codon
Δ*ftsW attB*$_{\Phi BT1}$::pMS82	DU548		cloning vector integrated by site specific recombination in DU521
Δ*ftsW attB*$_{\Phi BT1}$::pJS6 (*ftsW*$^{+}$)	DU550		pJS6 integrated at the ΦBT1 attachment site in DU521
Δ*ftsW attB*$_{\Phi C31}$::pKF280	DU584		*ypet* cloning vector integrated by site specific recombination DU521
Δ*ftsW attB*$_{\Phi C31}$::pKF351 (*ftsZ-ypet*)	DU586		*ftsZ-ypet* fusion vector integrated *in trans* by site specific recombination in DU521
Δ*ftsZ*::*apra*	DU500	DU669 [1]	844 bp deletion beginning 16 bp upstream of the *ftsZ* start codon
Δ*ftsZ*::*frt*	DU665		844 bp deletion beginning 16 bp upstream of *ftsZ* with insertion of 81 bp *frt* scar
Δ*ftsZ*::*apra attB*$_{\Phi BT1}$::pMS82	DU637	DU671	cloning vector integrated by site specific recombination in DU500/DU699
Δ*ftsZ*::*apra attB*$_{\Phi BT1}$::pJS8 (*ftsZ*$^{+}$)	DU536	DU670	*ftsZ*$^{+}$ genetic complementation vector integrated in *trans* in DU500/DU699
ftsZ2p::*apra*	DU504	DU505	6 bp deletion of the -10 site (TAGTGT) of a developmentally regulated promoter
*ftsZ*Δ*2p*	DU523		TAGTGT of -10 site of *ftsZ2p* replaced with ACTAGA
*ftsZ*Δ*2p attB*$_{\Phi BT1}$::pMS82	DU552		cloning vector integrated by site specific recombination in DU523
*ftsZ*Δ*2p attB*$_{\Phi BT1}$::pJS8 (*ftsZ*$^{+}$)	DU554		*ftsZ*$^{+}$ genetic complementation vector integrated *in trans* in DU523

†Unmarked gene deletions contain an in-frame six base scar (ACTAGA)

‡All strains were made for this study.

Table S2. Cosmids and plasmids used in the study

Vector/ construct	Description[†]	Reference or source
Sv-4-G01	Source of *ftsI*, *ftsL*, *ftsW*, *ftsQ*, and *ftsZ* (division and cell wall locus, *dcw*)	M. Bibb, unpublished
Sv-5-C06	Source of *divIC*	M. Bibb, unpublished
pIJ773	Source of *oriT apra* cassette	[2]
pIJ799	Source of cassette with *oriT apra* flanked with *bla* homology	[2]
pKF280	Control plasmid with promoter-less *ypet*, integrates at $attB_{\Phi C31}$ ($Apra^R$)	[3]
pKF351	Derivative of pKF280 containing *ftsZ-ypet*	[3]
pMS82	Cloning vector for genetic complementation, integrates at $attB_{\Phi BT1}$ (Hyg^R)	[4]
pJK1	Δ*ftsZ::apra-oriT*, Sv-4-G01 derivative	This study
pJK3	*ftsZ*Δ*2p::apra-oriT*, Sv-4-G01 derivative	This study
pJK5	Δ*ftsI::apra-oriT*, Sv-4-G01 derivative	This study
pJK6	Δ*ftsL::apra-oriT*, Sv-4-G01 derivative	This study
pJK7	Δ*ftsW::apra-oriT*, Sv-4-G01 derivative	This study
pJK9	Δ*ftsIL::apra-oriT*, Sv-4-G01 derivative	This study
pJK23	*ftsZ*Δ*2p bla::apra-oriT*, Sv-4-G01 derivative	This study
pJK26	Δ*ftsL bla::apra-oriT*, Sv-4-G01 derivative	This study
pJK27	Δ*ftsW bla::apra-oriT*, Sv-4-G01 derivative	This study
pJS6	pMS82 containing *ftsW* (5,434 bp *Pvu*II fragment)	This study
pJS7	pMS82 containing *ftsI* (5,686 bp *Pvu*II fragment)	This study
pJS8	pMS82 containing *ftsZ* (3,900 bp *Bam*HI-*Pst*I fragment)	This study
pJS10	pMS82 containing *ftsL* (2,869 bp *Kpn*I fragment)	This study
pJS18	Δ*divIC::apra-oriT*, Sv-4-C06 derivative	This study
pJS24	Δ*divIC bla::apra-oriT*, Sv-4-C06 derivative	This study
pJS26	pMS82 containing *divIC* (679 bp PCR fragment beginning 187 bp upstream of *divIC*)	This study
pJS30	Δ*ftsQ::apra-oriT*, Sv-4-G01 derivative	This study
pJS32	pMS82 carrying P_{dcw}-*ftsQ* (1095 bp PCR fragment containing 257 bp of *Pdcw* and *ftsQ*)	This study
pJS39	Δ*ftsQ bla::apra-oriT*, Sv-4-G01 derivative	This study
pJS40	Δ*ftsZ::frt bla::apra-oriT*, Sv-4-G01 derivative	This study
pJS41	Δ*ftsI::frt bla::apra-oriT*, Sv-4-G01 derivative	This study

[†]Apr^R, apramycin resistance; Hyg^R, Hygromycin resistance; Unmarked gene deletions contain an in-frame six base scar (ACTAGA)

Table S3. Oligonucleotides used in this study

Name	Sequence	Application
SVftsZ60	GCGGCGCGAACCAACGCGCGGCGACGACACGTA ACTCGAGATTCCGGGGATCCGTCGACC	*ftsZ* deletion in cosmid Sv-4-G01
SVftsZ59	TGATGTTGGCCTCGGGGTGGGCGGCCTCGCTGAC CAGCTGTGTAGGCTGGAGCTGCTTC	
SV2pUP66	AGGTTCGGCGTGTTCGTTGAACGTGCGCCACTTG TCGACT**ACTAGT** ATTCCGGGGATCCGTCGACC	*ftsZ2p* “-10” deletion in cosmid Sv-4-G01
SV2pDOWN65	GGTTACCAGTGTCTCTGTTCGCTGGACTCTTCCG AACAGG**TCTAGA** TGTAGGCTGGAGCTGCTTC	
SVftsL64	CGGGGCGCCGAGCGGATCCGGGAAGACGTCCAG TGAGC**ACTAGT**ATTCCGGGGATCCGTCGACC	*ftsL* deletion in cosmid Sv-4-G01
SVftsL65	CCGGCTTCGAGGGCGTCGGGGACGGCTTCGGGG CCTCCGC**TCTAGA**TGTAGGCTGGAGCTGCTTC	
SVftsW64	TCCACGAGCGGGCGCGGAAGGCCTGGGACCGGC CGCTC**ACTAGT**ATTCCGGGGATCCGTCGACC	*ftsW* deletion in cosmid Sv-4-G01
SVftsW63	CGGCGCAGGGCCAGGGCCGCTTTCGCGGCGGGT TCCTG**TCTAGA**TGTAGGCTGGAGCTGCTTC	
SVftsI60	GCGCCGCCGCGTTCCCGGACCCGCCCGGCCCGC GCGCCCCATTCCGGGGATCCGTCGACC	*ftsI* deletion in cosmid Sv-4-G01
SVftsI59	GCGTCAGGTACCAGGTCTCGTGGTCGACGTCGTC CTTGAATGTAGGCTGGAGCTGCTTC	
ftsQSXFor	AGGCGTAGCGCGGCGGCTGAGGGCAGGAGGCGC CAGGTG**ACTAGT**ATTCCGGGGATCCGTCGACC	*ftsQ* deletion in cosmid Sv-4-G01
ftsQSXRev	CTGGCCAACCAGGGTGCTGGCCAGGGGTGATAC CCGTCA**TCTAGA**TGTAGGCTGGAGCTGCTTC	
divICSXF	GTGCGGGGACGTCCGCGTGAACAGGGGAGGCGA CACGAC**ACTAGT**ATTCCGGGGATCCGTCGACC	*divIC* deletion in cosmid Sv-5-C06
divICSXR	TTCTCTCGGTTGCCTTGCTCGTCTGGTGCGGAGG AGGGG**TCTAGA**TGTAGGCTGGAGCTGCTTC	
SVdcwPSXF	CGCTCGCCCGTACCTCCGCGCCGGATCTGAGAG GGCGCA**ACTAGT**ATTCCGGGGATCCGTCGACC	Unmarked deletion of *dcw* locus between *Pdcw* and *ftsQ* in cosmid Sv-4-G01
SVdcwPSXQR	CGCGCCGCTCTTCTCGGCGGTCGTCGGTCCGGCT GCCAC**TCTAGA**TGTAGGCTGGAGCTGCTTC	
22ftsQEcoRV	GGAATTC**GATATC**GAGGGGACAAAGAACCGCAT	PCR amplify *Pdcw*- *ftsQ* for complementation
22ftsQSpeI	GGAATTC**ACTAGT**GCTGGCCAGGGGTGATACCC	
divICcompEcoRV	GGAATTC**GATATC**CATCGAGGAGATCCTCGAC	PCR amplify *divIC* with native promoter for complementation
divICcompSpeI	GGAATTC**ACTAGT**GTTTCTCTCGGTTGCCTTGC	

Figure S1

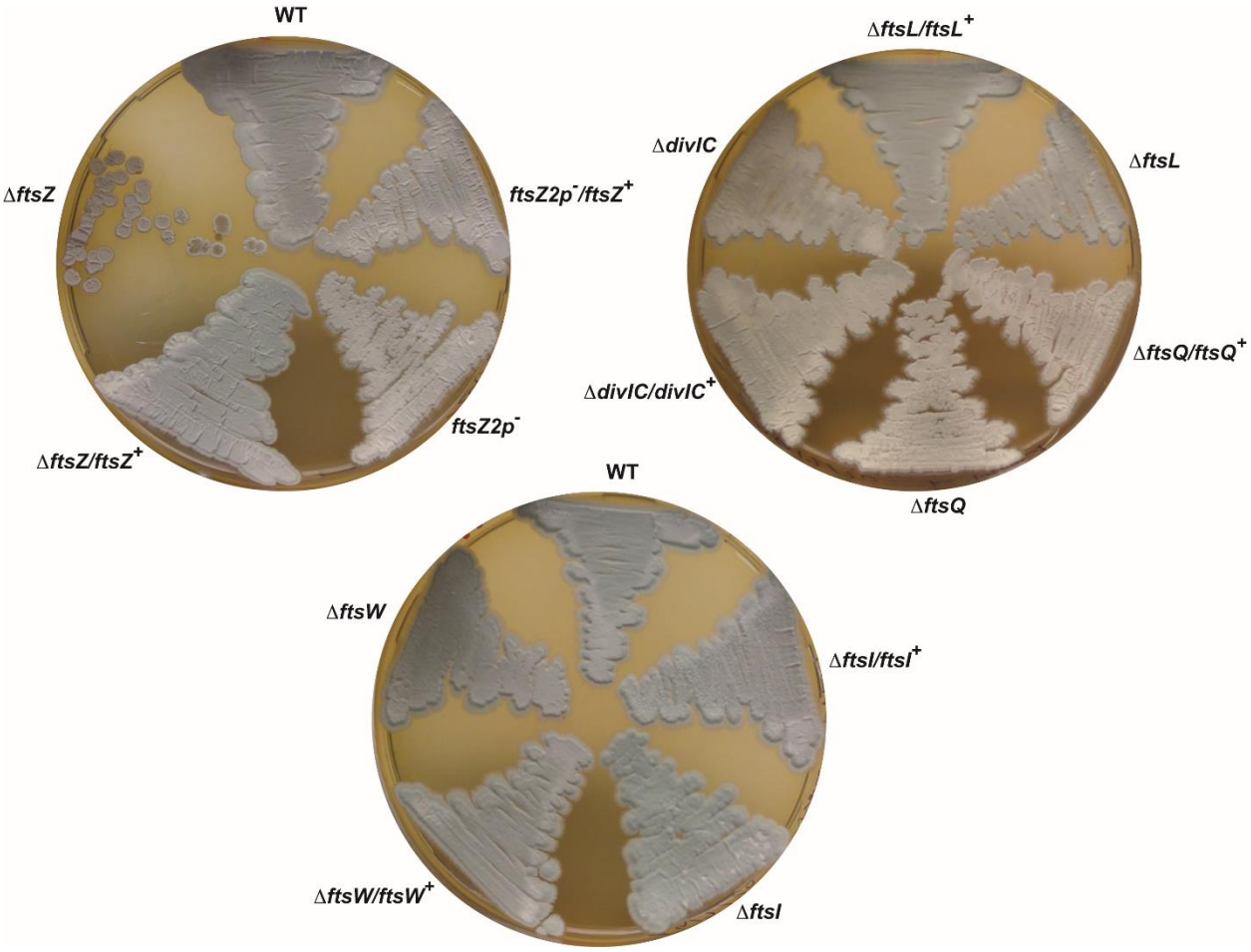

Figure S1. Macroscopic phenotypes of isolated *S. venezuelae* cell division mutants. Shown are patches of wild type *S. venezuelae* ATCC 10712 and congenic divisome mutant strains after growth on MYM agar for 4 days at 30°C. Pairs of mutant strains are shown containing either empty integration vector (pMS82) or a cognate genetic complementation vector, respectively. The wild type parent strain shown also contains the empty vector pMS82 (WT).

Figure S2

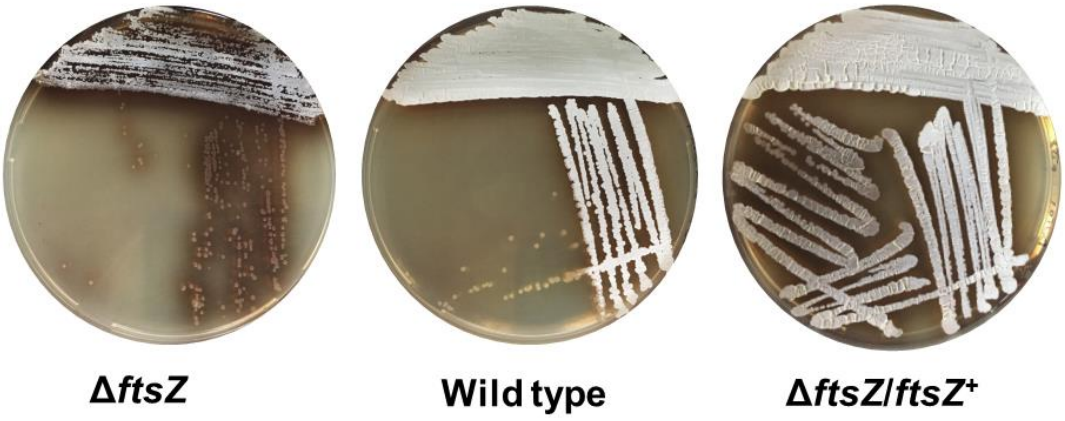

Figure S2. Colony phenotypes of *ftsZ*-null mutant, complemented null mutant and wild type strains.
Shown are streak plates of *ftsZ*-null mutant (DU500), wild type and *ftsZ*-null mutant containing the genetic complementation vector pJS8 (DU537) grown for 2 days on MYM agar at 30°C.

Figure S3

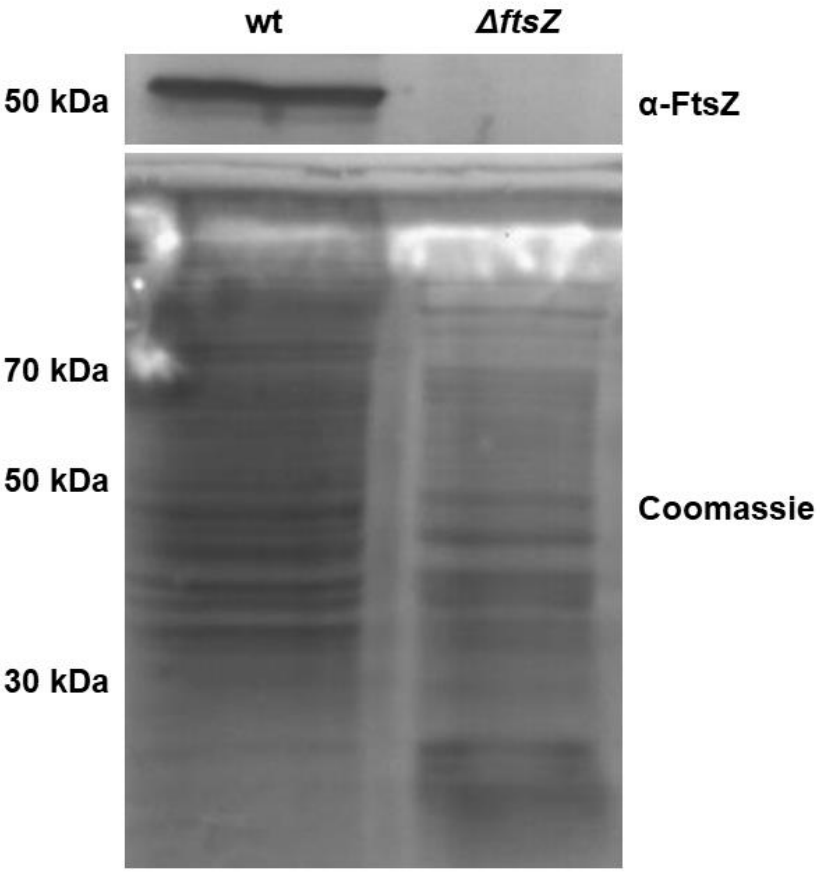

Figure S3. Western blot analysis of wild type and *ftsZ*-null mutant strains using polyclonal anti-FtsZ antibody.
Cultures of wild type and *ftsZ*-null mutant (DU500) were grown overnight in MYM liquid medium. Cell extracts were obtained by bead mill homogenization and normalized amounts of total protein was fractionated in duplicate on 12% polyacrylamide-SDS gel. Fractionated proteins were either stained with Coomassie brilliant blue (lower panel) or transferred to a solid support for a western blot analysis (upper panel). FtsZ was detected using a polyclonal antibody raised against FtsZ from *S. coelicolor* [5] and a secondary antibody conjugated with alkaline phosphatase.

Figure S4

(a)

```
S. venezuelae    CGGGTATcacccCtGGCCAGCACCCTGGTTGGcCAGCGCTACGGgTGATCACATAGGG    58
S. coelicolor  gaCGGGTATacgtgCaGGCCAGCACCCTGGTTGGgCAGCGCTACGGcTGATCACATAGGG    60
                         ftsZ3p
                          ##
S. venezuelae  TGAAAAGAAAAACGGGAGGTTCGGCGTGTTCGTTGAACGTGCGCCACTTGTCGACTTAGT   118
S. coelicolor  TGAAAAGAAAAACGGGAGGTTCGGCGTGTTCGTTGAACGTGCGCCACTTGTCGACTTAGT   120

                       ftsZ2p                                        ftsZ1p
                        ###                                           ##
S. venezuelae  GTCCTGTTCGGAAGAGTCCAgcGAACAGAGACACTGGTAACCCTAAACTTCAaCGTTAGG  178
S. coelicolor  GTCCTGTTCGGAAGAGTCCAagGAACAGACACACTGGTAACCCTAAACTTCAgCGTTAGG  180


S. venezuelae  GTTtGGGTCGGCGtTtCGGACCGTCCCAATCGGCATCcGTCGgaGcGgCGCGa    AcC  234
S. coelicolor  GTTcGGGTCGGCGcTaCGGACCGTCCCAATCGGCATCaGTCGtcGgGtCGCGggggcAtC  240


S. venezuelae  AacGCgcgGcgac      GACACGTAACTCGAGGCGAGAGGCCTTCGAC            278
S. coelicolor  AgtGCttcGgcggCCGGGCGACACGTAACTCGAGGCGAGAGGCCTTCGAC            290
```

(b)

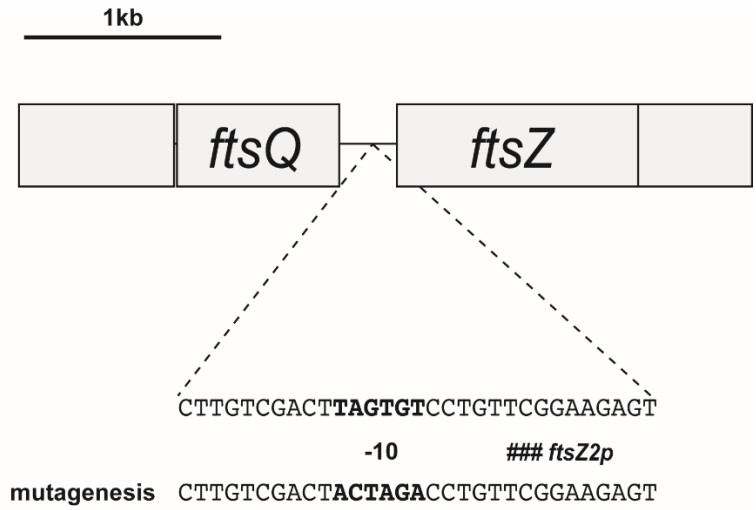

Figure S4. Comparison of the nucleotide sequences for *S. coelicolor* and *S. venezuelae ftsQ-ftsZ* intergenic regions containing the developmental *ftsZ2p* promoter and the sequence of the constructed *S. venezuelae ftsZ2p* promoter mutation.
(a) Nucleotide sequences of the entire intergenic regions upstream of *ftsZ* from *S. venezuelae* (278 bases) and *S. coelicolor* (290 bases) were aligned and the 3 promoters mapped in *S. coelicolor* are indicated (hash marks and bolded transcription start sites). Conserved sequences are in capital letters and divergent sequences are in small letters. (b) Five of the six residues at the -10 sequence of *ftsZ2p* (TAGTGT) for *S. venezuelae* were mutated to ACTAGA in this study (-10 sequences are bolded). The introduction of this *ftsZΔ2p* mutation into *S. venezuelae* ATCC 10712 created strain DU523.

Figure S5

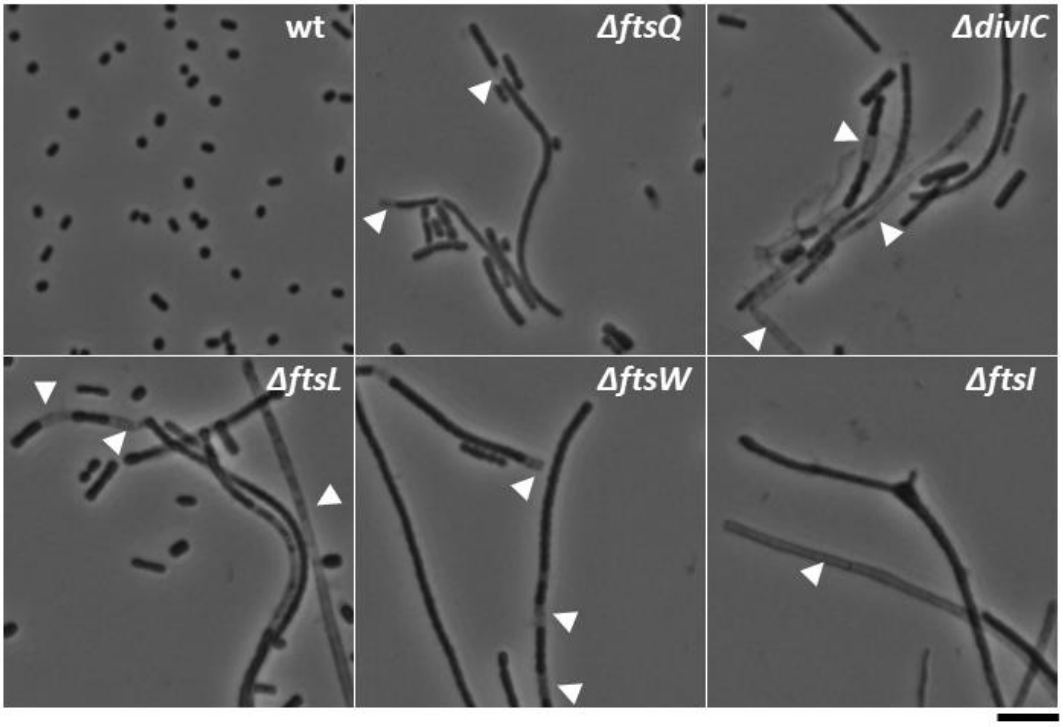

Figure S5. Spores and aerial hyphae are less robust in mutants for *ftsQ*, *ftsL*, *divIC*, *ftsW* and *ftsI* than in the wild type.
Strains were grown for 4 days on MYM agar at 30°C. Impression coverslip lifts were prepared and representative phase-contrast micrographs are shown for wild type and mutant strains. Arrowheads indicate frequent lysed regions of hyphae and spore compartments for the mutants, which are not typically observed for the wild type. Scale bar, 5 µm.

Figure S6

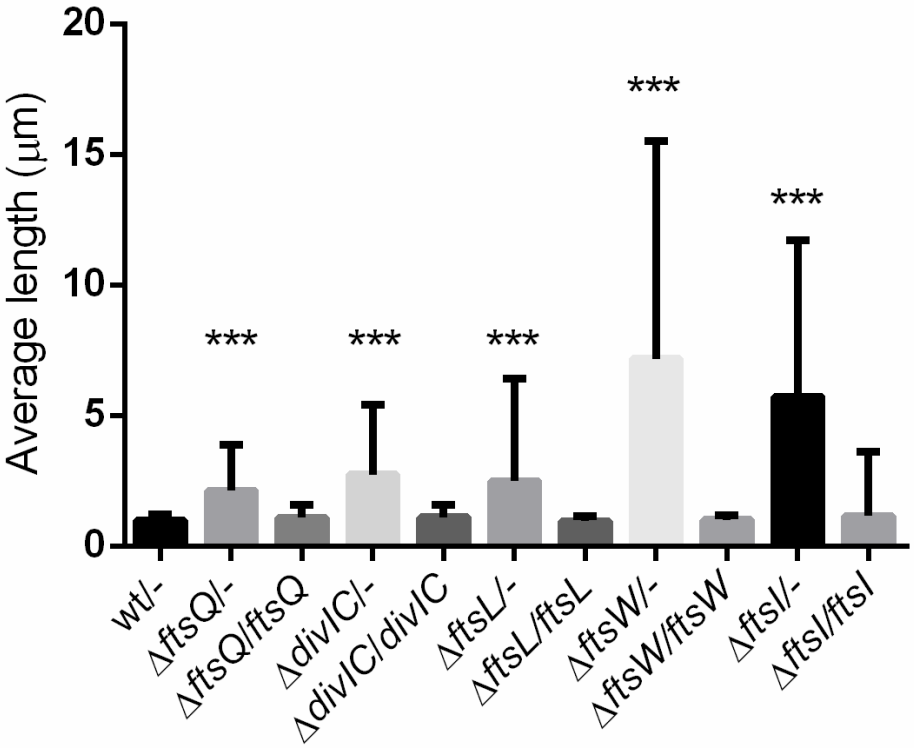

Figure S6. The average length of mature spore and spore-like cells resulting from completed development-associated division events from wild type and mutant strains. Strains were grown for 4 days on MYM agar and spores and spore-like cells were harvested in a standard fashion. Samples for the wild type, containing pMS82 (empty vector), and mutant strains, containing either pMS82 or a genetic complementation vector containing the cognate divisome gene, were spotted onto pads of 1% agarose and images were captured by phase-contrast microscopy. The lengths of spores and spore-like cells were measured. The data represent averages from 3 technical replicates. Bars show the standard deviation. For each strain, N = 750. A one-way ordinary ANOVA analysis with Dunnett's multiple comparisons test showed that the mutants all differ from the wild type with $p<0.0001$. The average spore length of each divisome mutant is significantly different from the wild type while the average spore length of each complemented strain is not.

Figure S7

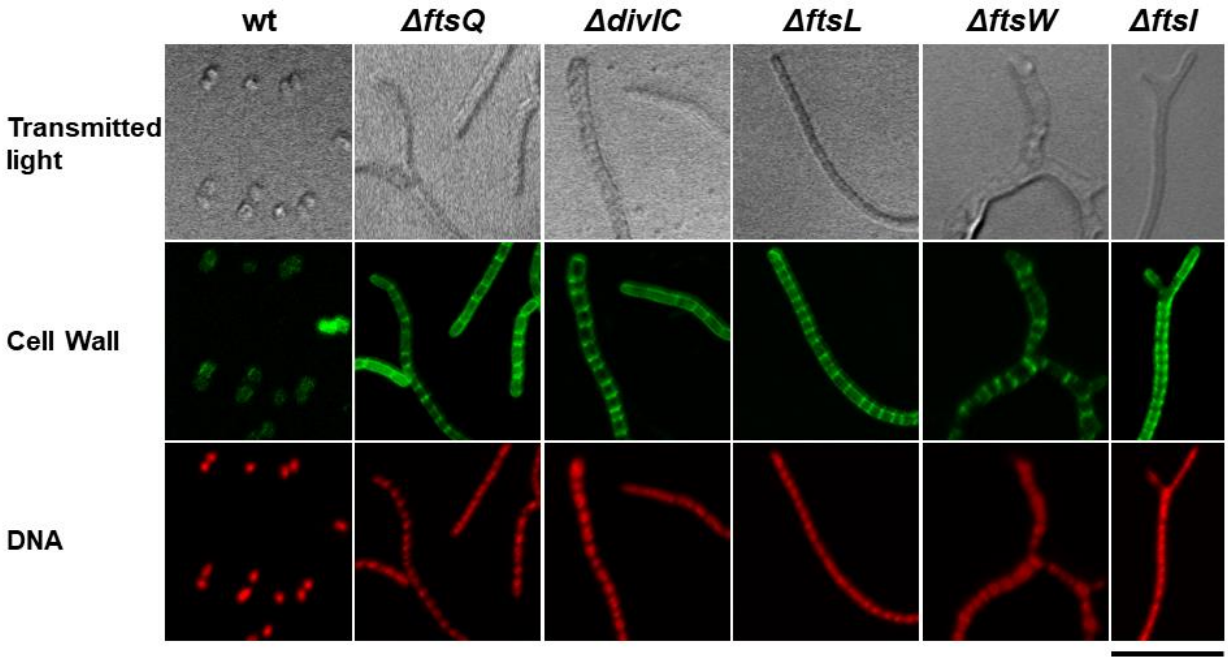

Figure S7. Developmental genome segregation is not overtly affected in core divisome mutants.
Strains were grown for 2 days on MYM agar at 30°C and impression coverslip lifts were made. The top row contains corresponding DIC light images. Samples of aerial hyphae were stained for cell wall (green) and DNA (red) and viewed by epifluorescence microscopy. Wild type samples contained mainly spores. Examples of aerial hyphae of mutant strains are shown. Aerial hyphae of the mutants typically contain segregated nucleoids with few anucleate compartments. Scale bar represents 5 μm.

Figure S8

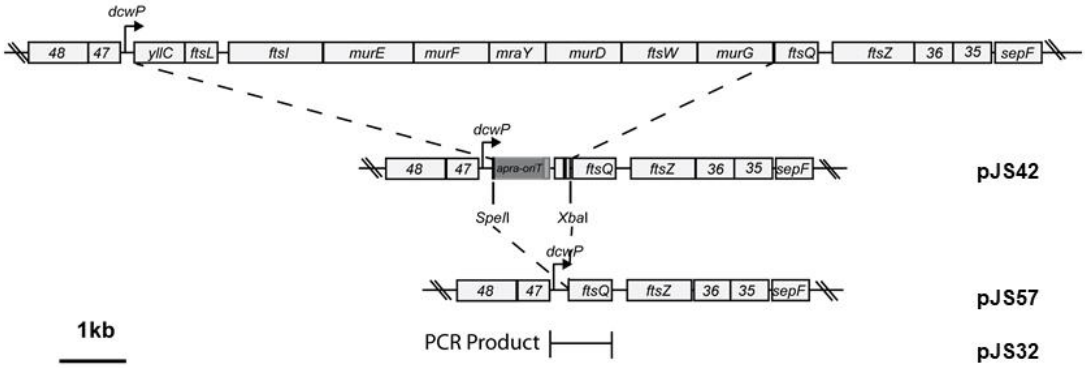

Figure S8. Intermediate plasmid constructions used to make a complementation plasmid for a Δ*ftsQ* mutant.

A complementation plasmid was constructed to put expression of the *ftsQ* gene directly under the control of the native *dcw* locus promoter (pJS32). Starting with cosmid Sv-4-G01, recombineering was used to delete 9 *dcw* genes located between *ftsQ* and the *dcw* promoter generating pJS42. The unique *Spe*I and *Xba*I restriction sites, introduced in the process of making pJS42, were digested and religated resulting in pJS57. pJS57 was used as template for PCR to generate complementation plasmid pJS32.

Movie legends

Movie S1: Time-lapse fluorescence microscopy of FtsZ-YPet in sporulating wild-type *S. venezuelae*. Shown is a time-lapse microscopy experiment consisting of fluorescence images of FtsZ-YPet (right) and the corresponding phase-contrast images (left) of DU578 (*ftsZ*$^+$ *attB*$_{\phi C31}$*::*pKF351[*P*$_{ftsZ}$-*ftsZ-ypet*]). Cells were grown at 30°C in MYM medium in a microfluidic system and monitored by fluorescence microscopy. After an initial period (4-6 hours) of vegetative growth, spent medium was administered to induce sporulation. The time interval between each frame is 10 min. Experiment was run two times. Scale bar, 2 µm.

Movie S2: Time-lapse fluorescence microscopy of FtsZ-YPet in sporulating *S. venezuelae* *ΔftsQ* mutant. Shown is a time-lapse microscopy experiment consisting of fluorescence images of FtsZ-YPet (left) and the corresponding phase-contrast images (right) of DU633 (*ΔftsQ* *attB*$_{\phi C3}$*::*pKF351[*P*$_{ftsZ}$-*ftsZ-ypet*]). Cells were grown at 30°C in MYM medium in a microfluidic system and monitored by fluorescence microscopy. After an initial period (4-6 hours) of vegetative growth, spent medium was administered to induce sporulation. The time interval between each frame is 10 min. Experiment was run two times. Scale bar, 5 µm.

Movie S3: Time-lapse fluorescence microscopy of FtsZ-YPet in sporulating *S. venezuelae* *ΔftsW* mutant. Shown is a time-lapse microscopy experiment consisting of fluorescence images of FtsZ-YPet (right) and the corresponding phase-contrast images (left) of DU586 (*ΔftsW* *attB*$_{\phi C31}$*::*pKF351[*P*$_{ftsZ}$-*ftsZ-ypet*]). Cells were grown at 30°C in MYM medium in a microfluidic system and monitored by fluorescence microscopy. After an initial period (4-6 hours) of vegetative growth, spent medium was administered to induce sporulation. The time interval between each frame is 10 min. Experiment was run two times. Scale bar, 5 µm.

Supplementary references

1. **Santos-Beneit F, Roberts DM, Cantlay S, McCormick JR, Errington J.** A mechanism for FtsZ-independent proliferation in *Streptomyces*. *Nat Commun*. 2017;8:1378. Doi: 10.1038/s41467-017-01596-z
2. **Gust B, Challis GL, Fowler K, Kieser T, Chater KF.** PCR-targeted *Streptomyces* gene replacement identifies a protein domain needed for biosynthesis of the sesquiterpene soil odor geosmin. *Proc Natl Acad Sci USA*. 2003;100:1541-6. Doi: 10.1073/pnas.0337542100
3. **Donczew M, Mackiewicz P, Wrobel A, Flärdh K, Zakrzewska-Czerwinska J, Jakimowicz D.** ParA and ParB coordinate chromosome segregation with cell elongation and division during *Streptomyces* sporulation. *Open Biol*. 2016;6:150263. Doi: 10.1098/rsob.150263
4. **Gregory MA, Till R, Smith MC.** Integration site for *Streptomyces* phage phiBT1 and development of site-specific integrating vectors. *J Bacteriol*. 2003;185:5320-3. Doi: 10.1128/jb.185.17.5320-5323.2003
5. **Schwedock J, McCormick JR, Angert EA, Nodwell JR, Losick R.** Assembly of the cell division protein FtsZ into ladder-like structures in the aerial hyphae of *Streptomyces coelicolor*. *Mol Microbiol*. 1997;25:847-58. Doi: 10.1111/j.1365-2958.1997.mmi507.x